AN ABSTRACT OF THE THESIS OF

Melissa D. Frey for the degree of Master of Science in Atmospheric Science presented on March 8, 2007.

Title: Development of a Synoptic Map-Pattern Climatology to Supplement Current Weather Forecasting Methods

Abstract approved:

____

Michael H. Unsworth

Many meteorologists rely heavily on their experience of past weather events to supplement their forecasting tools, such as using past experience to help decide between conflicting numerical weather prediction models. Experiential knowledge is an important piece of forecasting, however it is highly subjective and variable from one forecaster to another. In efforts to replace this experiential knowledge with a more objective record, this thesis explains how a synoptic map-pattern climatology was created and how it could be used as a contribution to weather forecasting methods.

Creating the map-pattern climatology was a two step process: first atmospheric flow patterns at the 500-millibar level for the selected region were categorized by type; and second surface level weather data were correlated with the map-types found. The atmospheric flow patterns over the Pacific Northwest region were found using a correlation-based method. Each day during the winter months of December, January, and February for the past 58 years was categorized by map-type. This resulted in 5,235 days that were classified into 20 distinct map-type groups. Once the map-types were found, temperature, precipitation, and snowfall data from stations throughout Oregon and Washington were then correlated to the map-type data. The weather data were calculated for three spatial scales: an average of Oregon and Washington combined; average by Oregon climate zone; and for a single city. It was found that each map-type is associated with a unique weather environment at the surface. As an additional study, the distribution of map-types during El Niño and La Niña years was studied in combination with the surface weather data. It was found that El Niño and La Niña years have quite different map-type distributions compared to normal years, and the weather resulting at the surface was also far from average.

Once completed, this Pacific Northwest climatology provided a record of the most common flow patterns and resulting weather at the surface. If distributed in a format in which current atmospheric flow data could be compared to historical map-type data, this synoptic map-pattern climatology could be used as a forecasting tool. In order for this information to replace the previously relied upon experiential knowledge, it would be necessary to know the forecast day's projected map-type along with the historical surface weather data associated with that map-type. If distributed in this way, weather forecasters would have easy access to what has happened historically with any given map-type, thus replacing their variable and subjective experiential knowledge with an objective and accurate record.

Development of a Synoptic Map-Pattern Climatology to Supplement Current Weather Forecasting Methods

By
Melissa D. Frey

A THESIS

submitted to

Oregon State University

in partial fulfillment of
the requirements for the
degree of

Master of Science

Presented March 8, 2007

Commencement June 2007

Master of Science thesis of Melissa D. Frey presented on March 8, 2007.

APPROVED:

Major Professor, representing Atmospheric Sciences

Dean of the College of Oceanic and Atmospheric Sciences

Dean of the Graduate School

I understand that my thesis will become part of the permanent collection of Oregon State University libraries. My signature below authorizes release of my thesis to any reader upon request.

Melissa D. Frey, Author

ACKNOWLEDGEMENTS

There are many people I have to thank for contributing to this thesis and my education here at Oregon State University. The instruction I have received about atmospheric science and the process of scientific research in my time here is invaluable and will surely shape the years to come.

I would like to thank my advisor Dr. Mike Unsworth for his generous guidance and support from day one. I would not be completing this degree had it not been for his genuine words of encouragement and advice throughout the process. His countless hours reviewing my research and thesis are much appreciated.

I would also like to thank George Taylor for taking me under his wing and allowing me to work on this exciting project. His genuine enthusiasm for climatology and meteorology were a treat to be around. This thesis was made possible through his generous contributions of data, guidance and financial support of which I am very thankful.

Thanks to Drs. Chris Daly, Eric Skyllingstad and Todd Palmer for serving on my committee and examining this thesis. I am grateful for Wayne Gibson and all his help with programming and technical difficulties, for all of my fellow classmates, whose scientific discussions over class material greatly contributed to my learning and made this process more enjoyable and for Lori Hartline, Robert Allen and Bob

Duncan of Student Programs for their continual efforts to guide and support students, as I know I was, so that they may receive the best possible education.

I would like to thank my parents, friends, and family members who offered me endless support, encouragement and advice through this process. Their efforts and prayers made this dream a reality. Finally, I would like to express my sincere gratitude to my husband Tim who contributed to this thesis both directly and indirectly. This research would not have been possible without his generous programming contributions. I am thankful for his wise counsel about the scientific method, willingness to support me during this endeavor, and empathy day in and day out.

TABLE OF CONTENTS

Page

TABLE OF CONTENTS (Continued)

Page

LIST OF FIGURES

LIST OF FIGURES (Continued)

Figure | Page

LIST OF FIGURES (Continued)

Figure Page

LIST OF FIGURES (Continued)

LIST OF FIGURES (Continued)

Figure Page

LIST OF FIGURES (Continued)

Figure Page

LIST OF TABLES

LIST OF TABLES (Continued)

Table Page

Development of a Synoptic Map-Pattern Climatology to Supplement Current Weather Forecasting Methods

1 Introduction

1.1 Motivation

More than 100 million U.S. households obtain weather forecasts at least once every day (Weiher 2006), a logical number given the estimated 2.2 trillion dollars that are lost each year in the U.S. from the impact of weather related events (Hernandez 2001). Improving the accuracy of weather forecasting has been a goal of meteorologists for over 2000 years. In the last 50 years, computers have become 100 million times faster, allowing a worldwide network of atmospheric data to be continually processed, giving us more precise and reliable forecasting methods. Computer technology, however, is only as sophisticated as its programmer, and as creative as its user.

Due to the dynamic nature of the atmosphere and the shortcomings that all forecasting methods have, the accuracy of weather forecasting will not improve by merely maintaining the current tools, but rather by working to improve the range of tools available. Many weather forecasters rely on a combination of numerical weather prediction models along with their experience and knowledge of a region. This experiential knowledge is often what sets established forecasters apart from the beginners. Forecasters who are able to remember and catalog the correlation between a particular flow pattern and the impact it has had at the surface are likely to have a better chance at a successful forecast. Although, relying on subjective methods creates significant variability even between experienced forecasters. This reliance of an entire scientific field on subjective methods suggests a need for something more objective. Creating an objective method, which represents the experience one gains from forecasting in the same region for an extended period, would greatly enhance the field of weather forecasting.

The catalog of information that established forecasters have about the weather of a particular region is essentially a partially memorized synoptic map-pattern climatology. Synoptic map-pattern climatologies are developed by classifying atmospheric circulation types and then assessing a relationship between these types and the region’s weather (Barry and Perry 1973). Once created, a synoptic climatology can provide a great deal of information about the region in which it is created. If one believes that history repeats itself, this objective record of atmospheric circulations, and the corresponding surface data, will have the potential to diversify current forecasting tools. Though the concept of synoptic climatologies has been around for several decades, due to the lack of technology available they have never been created for a large historical record and then made readily available as a forecasting tool. The aim of this research is to explore the possibility of transforming a widely used subjective method into an objective tool. This will be accomplished by developing a synoptic map-pattern climatology of the Pacific Northwest.

1.2 Overview of the Study

The next two chapters of this thesis provide a background of synoptic map-pattern climatologies. Chapter 2 provides a short explanation of 500-millibar maps and how they relate to flow in the atmosphere. Literature on map-pattern climatologies is reviewed in Chapter 3, looking at the history of synoptic climatology and its application in previous studies. Based on background information given in Chapters 2 and 3, Chapter 4 formulates the design of a map-pattern climatology, leading to Chapter 5, which explains the results of the first step of the climatology. The second step of the climatology is presented in Chapter 6, where the results of the map pattern classifications presented in Chapter 5 are related to the surface environment. Connections between the map patterns and surface observations are then discussed and conclusions are drawn in Chapter 7.

2 Upper Air charts: 500-millibar maps and their relation to atmospheric flow

According to Barry and Perry (1973), every synoptic climatology has two stages: classifying atmospheric circulations into categories and then assessing the weather associated with each category. Atmospheric circulations, used in the first stage, are most easily identified on 500-millibar maps. These maps show the wind-flow and pressure patterns aloft, helping forecasters to understand the movement of weather systems and the development of weather systems at the surface.

Commonly referred to as upper-air charts, these maps show the contours of the 500-millibar level. The 500-millibar level is located roughly half-way through the troposphere, or about 5.5 km above sea level. Twice a day, radiosondes are launched from sites all over the globe. As this weather instrument ascends through the atmosphere it collects pressure, temperature and humidity values, and transmits them back to the surface. The height at which the balloon reaches the 500-millibar level is recorded. This height, which is the distance between a mean surface level and the 500-millibar level, is expressed as the geopotential height. Maps of the 500-millibar level are therefore contour plots of the geopotential height, a variable often used in atmospheric calculations.

Winds at the surface and throughout the troposphere are controlled by Newton's first two laws of motion (Ahrens 2000). These laws state that an object in motion remains in motion until a force is exerted on it and the force is equal to the mass times the acceleration. Applying Newton's laws to the atmosphere, we know that air will accelerate in the direction in which a resultant force is acting.

Two forces, the pressure gradient force and the Coriolis force affect the linear flow of air traveling at the 500-millibar level. The pressure gradient force, which occurs any time there is a difference in pressure between two locations, causes the wind to blow. The pressure gradient force acting on a given mass of air directs the wind from higher pressure to lower pressure; the stronger the pressure gradient, the stronger the force. If this were the only force, then the wind would always blow directly from high-pressure areas to low pressure areas. The other force affecting the wind is the Coriolis force, an apparent force that is due to the effects of the earth rotating. Any freely moving object, including an air parcel, is deflected to the right (in the Northern Hemisphere) of its otherwise straight path due to the earth continuing to rotate beneath it. The Coriolis force pulls the wind at a 90-degree angle to the right of the pressure gradient.

When the force system acting at the 500-millibar level is in equilibrium, the Coriolis and pressure gradient forces are equal and opposite, known as geostrophic balance, and the wind blows at a 90 degree angle to the right of the pressure gradient in the northern hemisphere. Thus, the wind blows parallel to the lines of constant pressure, or in this case, the lines of constant height, which is known as geostrophic flow (See Figure 2.1).

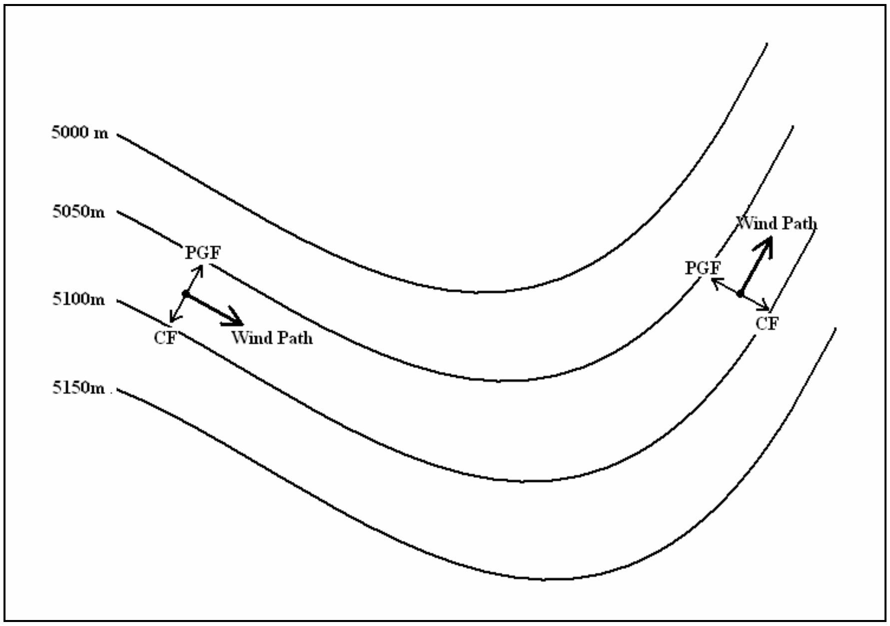

Figure 2.1: Example of a 500-mb map. The wind path is blowing parallel to the lines of constant pressure due to the balance between the pressure gradient force and Coriolis force resulting in geostrophic flow.

Most flow at the 500-millibar level in the middle latitudes is geostrophic, although, a third force may be introduced around sharp troughs in the flow;

> Within sharp troughs in the middle-latitude westerlies, the observed velocities are often subgeostrophic by as much as 50%, even though the streamlines still tend to be oriented parallel to the isobars. These large departures from geostrophic balance are a consequence of the large centripetal acceleration associated with the sharply curved flow within such regions (Wallace and Hobbs 1977).

The consequence of large centripetal acceleration results in a centrifugal force which is always directed “outward from the center of curvature of the air trajectories” (Wallace and Hobbs 1977). In the case of cyclonic flow, the centrifugal force is in the same direction as the Coriolis force, and therefore pulls the air parcel away from the center of rotation. This results in a decrease of the centrifugal force as the parcel has moved further from the center of rotation and the pressure gradient force becomes the dominant force, pulling the air parcel back toward the center of rotation. This constantly changing balance of forces causes the air to travel parallel to the isobars, or lines of constant height, only at a smaller velocity than the purely geostrophic case when the Coriolis force is the only force balancing the pressure gradient force.

Therefore, any time we look at a 500-millibar map it is not only a pressure chart, but it also displays the path of the wind at this level in the atmosphere. Understanding the velocity and trajectory of the wind provides forecasters with information about each weather system. As is described in the following chapter, upper air charts have been used in creating climatologies for many years.

3 Historical Development of Synoptic Climatology

Synoptic climatology is a branch of climatology that has significantly evolved over the past 60 years. As knowledge in meteorology and climatology progresses and with the ever-increasing speed and accessibility of computers, the applications and methods of developing synoptic climatologies continue to advance as well.

3.1 Definition of Synoptic Climatology

Synoptic Climatology is a term that was first used by W.C. Jacobs. Jacobs was head of the Special Studies Research Group within the Army Air Forces (AAF) Weather Service which was responsible for providing weather intelligence for all branches of the United States Army (Jacobs 1947). Wartime stresses enabled many scientific developments, including the advancement of both meteorology and climatology. Up-to-date and accurate weather and climate information was vital for planning military operations overseas. However, before any meteorological research could be conducted, the AAF Weather Service knew they first had to gather and store surface and upper-air data in a way that could easily be summarized and analyzed. The AAF instituted IBM punch-card facilities to code, punch and process weather data that could then be filed for later analysis. Although this new "Northern Hemisphere map series" provided an easily accessible record of climate data, it did not fulfill meteorologists' responsibility of providing weather intelligence to the military. Jacobs, along with other meteorologists, developed a synoptic or "synchronous" climatology to fulfill that responsibility. The steps of this climatology involved: (1) dividing up the geographical region of interest into smaller areas that could be “described by a single direction of gradient air flow” (Jacobs 1947); (2) examining historical weather maps and classifying them into groups; (3) gathering the surface weather data for each weather map; and (4) summarizing the data by correlating the surface weather data to the weather map groups found in step 2. This study was conducted for an eleven-year period. Jacob explained, “The synoptic climatology has served in a measure to break down the purely fictitious mean climatic picture into the individual, and real, weather patterns of which climate is composed” (1947). Jacobs further explained that this synoptic climatology was used mainly for strategic and tactical planning, but he believed it would also be useful as a forecasting tool, both for interpreting weather in areas where current weather information is limited and as an empirical forecast aid when used alongside a prognostic pressure chart (Jacobs 1947).

Ten years after Jacobs began his work in synoptic climatology, Arnold Court sought to bring about a more precise definition of the subject. Court explained that synoptic climatology developed out of using four different aspects of the weather map: the air flow, pressure-field, air-mass, and map pattern (Court 1957). He described each of these as being subdivisions of synoptic climatology: “air flow climatology”, “map pattern climatology”, etc. Court defined map pattern climatology as relating “surface weather conditions within an area to the general pressure and flow pattern over a much larger region.…The general flow patterns are classified into many types for each region" (Court 1957). He then provided a formal definition of synoptic climatology: "It describes the totality of weather resulting from, or at least physically related to, some aspect of the atmospheric circulation, as conveniently portrayed on a synoptic weather map" (Court 1957). Court was among the first to define synoptic climatology and remained among the few to do so for several years.

In 1973, a book was published by Roger Barry and Allen Perry, two scholars who recognized the need to further explain, teach and define synoptic climatology. In the preface of their book they explained, "Synoptic climatology is by no means a neat coherent field. Indeed, such is the variety of interpretation given to the term that it is in danger of becoming unusable. Hopefully this book may, as a byproduct, help to restore it as a recognized technical term" (Barry and Perry 1973). The efforts of these two authors to explain, teach and define had a significant impact in the field of climatology. To this day, much of the literature on synoptic climatology references Barry and Perry's book as a definitive source for both the history of synoptic climatology as well as an explanation of the data, methods and applications. Barry and Perry explained that there are two stages of climatology: "1-The determination of categories of atmospheric circulation type. 2-The assessment of weather elements in relation to these categories" (Barry and Perry 1973). Synoptic climatologists used this definition frequently and it remained unchanged for 20 years.

Following Barry and Perry's extensive contributions to synoptic climatology, the field continued to evolve with time. Due to the new developments and research in the field of synoptic climatology between 1973 and 1993, Brent Yarnal (Yarnal 1993) recognized a need for an updated synopsis of the field. Acknowledging the thorough work of Barry and Perry, Yarnal only focused on the previous two decades. One significant change in that time had been the broadening of synoptic climatology to encompass more aspects than just the weather. In the mid 1970's it became more common for synoptic climatologists to work with "non-meteorological but climatically-related variables such as surface ozone, crop yields, and water quantity and quality" (Yarnal 1993). In order to include such efforts, Yarnal redefined synoptic climatology to broaden its spectrum: "Synoptic climatology relates the atmospheric circulation to the *surface* environment" (1993). Several years later Yarnal refined his definition to focus more on the application of the climatologies rather than the methodology: "synoptic climatology integrates the simultaneous atmospheric dynamics and coupled response of the surface environment" (Yarnal, Comrie et al. 2002). Yarnal believed that although his first definition is and will continue to be applicable, it would be preferable if his new definition would take hold (2002).

As the methods and scope of synoptic climatology have evolved and expanded throughout the past 60 years, its definition has as well. Currently the accepted meanings of synoptic climatology are Barry and Perry's definition for fields in atmospheric science and Yarnal's first definition in all other areas.

3.2 Historical Methods and Applications of Synoptic Map-Typing Climatology

Several methods have been developed for creating synoptic map-typing climatologies. Due to the complex nature of the atmosphere, there are many ways one can classify atmospheric circulations into categories and correlate them to the surface environment.

Iver Lund was one of the first synoptic climatologists to design an objective map-pattern classification scheme. He sought to design an experiment to "explore the possibilities of applying simple linear correlation methods to the problem of identifying recurring map-pattern configurations" (Lund 1963). The dawn of computers enabled scientists to move away from subjective methods by being able to process larger amounts of data relatively quickly. Using data from 22 stations, Lund was able to classify the surface pressure over the western United States for five years of winter months. To classify the maps into groups, Lund first found a correlation coefficient for each set of maps using the Pearson product-moment correlation equation:

$$r_{xy} = \frac{\sum_{i=1}^{N} (x_i - \bar{x})(y_i - \bar{y})}{[\sum_{i=1}^{N} (x_i - \bar{x})^2 \sum_{i=1}^{N} (y_i - \bar{y})^2]^{1/2}}$$

where x_i represents the pressure of point N on the first map and y_i represents the pressure of point N on the second map; $\bar{x}$ and $\bar{y}$ represent the total mean of the N-point grid (Lund 1963). His classification scheme, which will be described in greater detail in Chapter 4, became a staple in synoptic map-pattern climatology. Lund transformed the difficult and subjective process of manual classification procedures into a simple and objective automated classification scheme. In the past 40 years, Lund's methods have been built upon and only slightly changed to fit the expanding needs of the science.

Six years after Lund's method was first expounded, Richard Augulis (Augulis 1969) put it to use. Using upper-level data on magnetic tape, Augulis executed a map-pattern climatology covering a seven-year period. With the help of slightly more advanced computers, Augulis was not only able to execute a longer period of record, but the data on record were more precise, making for more accurate map-types. The data Augulis used included 52 evenly spaced grid points, opposed to Lund's 22 unevenly spaced stations.

In the following decade several studies, including those of Rasch and MacDonald (1975) and Paegle and Kierulff (1974), were published using Lund's method to classify the atmosphere into map-types. Rasch and MacDonald (1975) investigated the probability of precipitation with each map-type, and found their results to be better than those from a simple climatology. Paegle and Kierulff (1974) used a map-pattern climatology to make a quasi-geostrophic model, calculating the probability of precipitation using linear regression equations. Although Lund's method was highly accepted and used regularly, a slightly altered method of correlating maps was introduced by Kirchhofer. This method became highly respected and perceived as superior to Lund's method (Willmott 1987). Rather than using the Pearson product-moment correlation equation as Lund did, Kirchhofer used a "sums-of-squares" algorithm to correlate the map patterns (Yarnal 1993). This equation is known as the Kirchhofer score:

$$S = \sum_{i=1}^{N} (Z_{xi} - Z_{yi})^2$$

where Z_{xi} represents the normalized grid value of point i on map x, Z_{yi} represents the normalized grid value of point i on map y and N is the number of points on each grid.

Even though these two techniques use different methods to correlate the maps in the data set, the results are found to be quite similar. Willmott (1987) showed that the Kirchhofer score could be derived from the Pearson product-moment correlation equation used by Lund. The Kirchhofer score and Lund's equation can be related to each other by the simple equation: $S = 2(1 - r)$. From this point on, it was seen that the Kirchhofer technique and the Lund technique were too similar to differentiate between the two. Yarnal suggested that such techniques should now be called "correlation-based" (Yarnal 1993).

As computer memory and speed continue to increase and the accessibility of accurate upper-air data also increases, synoptic map-pattern climatologies have become more accurate and functional in a variety of disciplines. In the last 20 years, several correlation-based map-typing studies have been reported. Such studies have been applied to boundary layer modeling (Hoard and Lee 1986), surface temperature variation over the Lake Superior Basin (Brinkmann 1999), studying precipitation, temperature and ENSO events in Southern South America (Bischoff and Vargas 2003), precipitation over watersheds of the Eurasian Arctic drainage system (Serreze and Etringer 2003) and to compare different global climate models (Schoof and Pryor 2004).

Although correlation-based map-typing climatologies have been effective for the needs of the above studies, the method has not been applied and made accessible for regional weather forecasting. This is the long-term objective of the work reported here.

4 Design of the Climatology

As shown in the previous chapter, there are many techniques and applications for developing synoptic climatologies. The desired result of the first stage of this synoptic climatology is a catalog of wind flow patterns that occur at 500-millibars over the Pacific Northwest. The method developed by Lund (1963) was the approach taken. The correlation-based map-pattern technique (Yarnal, 1993) is an automated method in which the criteria for the correlations are established beforehand. Though objective in nature, a few subjective choices are made throughout the study. These choices and the steps in creating the climatology are explained below.

4.1 Research Area

The research area for this study is a grid centered over the Pacific Northwest, stretching from 50N to 35N and from 140W to 115W (see figure 4.1). This 15^{o} by 25^{o} (roughly 1600 km by 2800 km) grid was chosen as it allows a focus on the atmospheric circulations over the Pacific Northwest while still picking up the large-scale flow over the Northeastern Pacific. Choosing a domain any larger would lose the focus on the Pacific Northwest and make it difficult to relate the map-typing data to the surface data. A smaller domain would be too small to accurately view and understand the flow pattern.

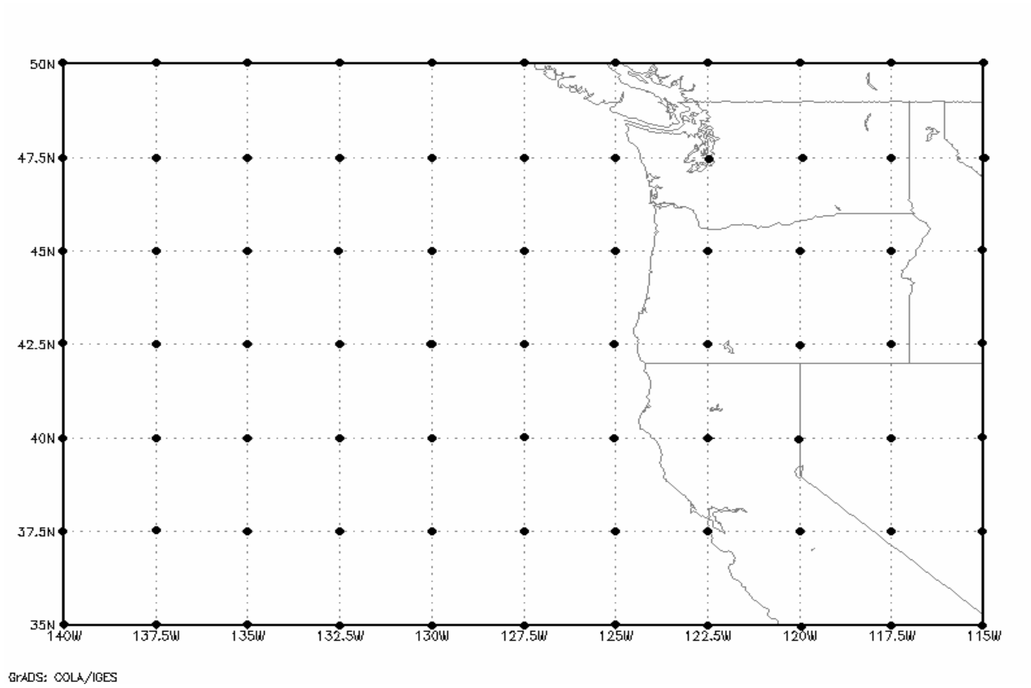

Figure 4.1: Research area covering 50N to 35N and 140W to 115W consisting of 77 grid points every 2.5˚.

4.2 Data

The 500-millibar geopotential heights used to produce this climatology were extracted from the NCEP/NCAR global reanalysis data set, a result of the combined efforts of the National Center of Environmental Protection and the National Center for Atmospheric Research. This record currently includes 58 years of "global analysis of atmospheric fields" (Kistler, Kalnay et al. 2001). After gathering surface, ship, rawinsounde, pibal, aircraft, satellite, and other data, quality control and assimilation procedures were executed to ensure the best possible accuracy for the data set (Kistler, Kalnay et al. 2001).

Data for the period of January 1948 through December 2005 were obtained from the NCEP/NCAR global reanalysis data set. Only the winter months (December, January and February) were considered to avoid seasonal variation in geopotential heights and to confine the scope of the study to only the most active months for synoptic disturbances. The resulting data set includes 5,235 days. After extracting the needed months, the data set was further reduced from a global record to the grid described in section 4.1 to focus on the selected region.

4.3 CALCULATING MAP CORRELATIONS

The first step in recognizing map-types is to correlate the geopotential heights at each of the points on each map with the corresponding heights on all the other maps in the data set. The “Pearson product-moment correlation” technique, where the similarity between map pairs is identified using the formula:

$$r_{xy} = \frac{\sum_{i=1}^{N} (x_i - \bar{x})(y_i - \bar{y})}{[\sum_{i=1}^{N} (x_i - \bar{x})^2 \sum_{i=1}^{N} (y_i - \bar{y})^2]^{1/2}}$$

were x_i represents the geopotential height of point N on the first map and y_i represents the geopotential height of point N on the second map; $\bar{x}$ and $\bar{y}$ represent the total mean of the N-point grid (Lund 1963). r_{xy}, known as the correlation coefficient for map x and map y, is found for every map pair in the data set.

4.4 Map Typing

After finding the correlation coefficients between every map pair, the map with the highest number of correlations above a set critical value is recognized. For this study, the critical value was chosen to be 0.8. Sabin (1974) found 0.8 to be the best critical value, allowing for a large number of map categories while still keeping a distinct and individual flow pattern for each category. Any two maps that have a correlation coefficient of greater than 0.8 are "significantly correlated" to each other.

The map with the most correlations above the critical value is the most common map pattern and is named the “key day” map for the most common class of maps. Once the first key day is determined, all of the maps that are significantly correlated with it are removed from the dataset. The second most common map pattern is then found and the maps that are significantly correlated with it are removed. This process is continued until twenty map type classes are found. For this study, the limit of twenty map-types was chosen as a balance between having enough map-types to recognize all of the significant flow patterns and having each map-type represent a specific and individual flow pattern.

In classifying all of the maps into their appropriate map-type category, all the maps that had a critical value above 0.8 with the current key day were removed each step of the way; however, these maps were never compared with the other map types that were subsequently found. Therefore, in a second stage of the analysis, the maps must be reclassified. In this step, every map is compared to the key day map representing each map-type group. Any maps that are found to have a higher correlation with another key day map are then reallocated into the map type group in which they have a stronger correlation. Figure 4.2 outlines this process.

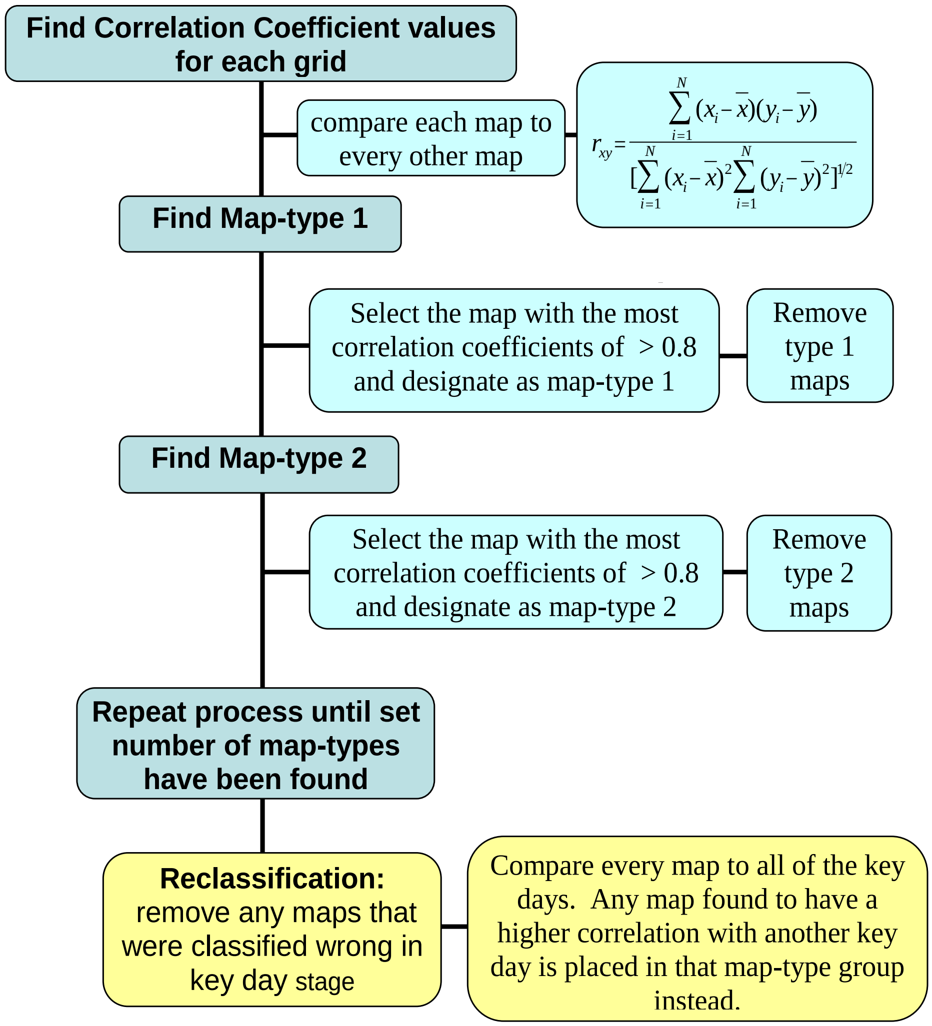

Figure 4.2: Flow chart showing map-typing process

The above steps were completed using a program written in C++. First, the 77 500-millibar geopotential heights, for each of the 5,235 days, were retrieved and provided input into the program, which then populated arrays with the data. The arrays allowed for comparison using the Pearson product moment correlation equation. For each of the 5,235 days analyzed, a 'struct' container stored the date, the date’s 77 data values and the assigned key day. The routine used ‘for-loops’ which were critical to the map-type and reclassification steps. Once the program completed the classification process outlined in figure 4.2, the information was outputted into a spreadsheet format for further analysis. This catalog of the twenty most common wind flow patterns that occur at 500 millibars over the Pacific Northwest, is presented in Chapter 5. These results represent the first half of the synoptic map-pattern climatology.

5 Results of Map-Typing

The product of this map-typing classification provides the twenty most common flow patterns seen over the Pacific Northwest during the winter months. Each of the twenty distinct map-types is represented by a key day, the day with the most significant correlations for that flow pattern. Table 5-1 and Figure 5.1 show the distribution of occurrence of the 20 map-types and the unclassified map group. The three most common map-types represent 59% of the 5235 days. Only 4.3% of the days were found unclassifiable into one of the 20 map-types.

The key day for each map-type group and the second two highest correlated maps for each map-type group are shown in Figures 5.2-5.22.

Table 5-1: Key day, number of maps in each group and frequency of occurrence.

Map Type	Key day	# of Maps in group	Frequency of Map Type
1	12/5/89	1544	29.5%
2	1/18/49	860	16.4%
3	12/13/69	699	13.4%
4	12/11/92	363	6.9%
5	1/31/01	237	4.5%
6	1/3/60	224	4.3%
7	1/20/76	162	3.1%
8	1/20/62	141	2.7%
9	1/25/69	131	2.5%
10	12/10/89	118	2.3%
11	1/8/98	95	1.8%
12	1/25/49	82	1.6%
13	1/6/57	73	1.4%
14	12/6/97	63	1.2%
15	1/20/60	51	1.0%
16	2/15/62	51	1.0%
17	1/21/61	39	0.7%
18	12/17/85	30	0.6%
19	1/6/77	26	0.5%
20	2/27/52	22	0.4%
0	Unclassified	224	4.3%
	Total	5235	100.0%

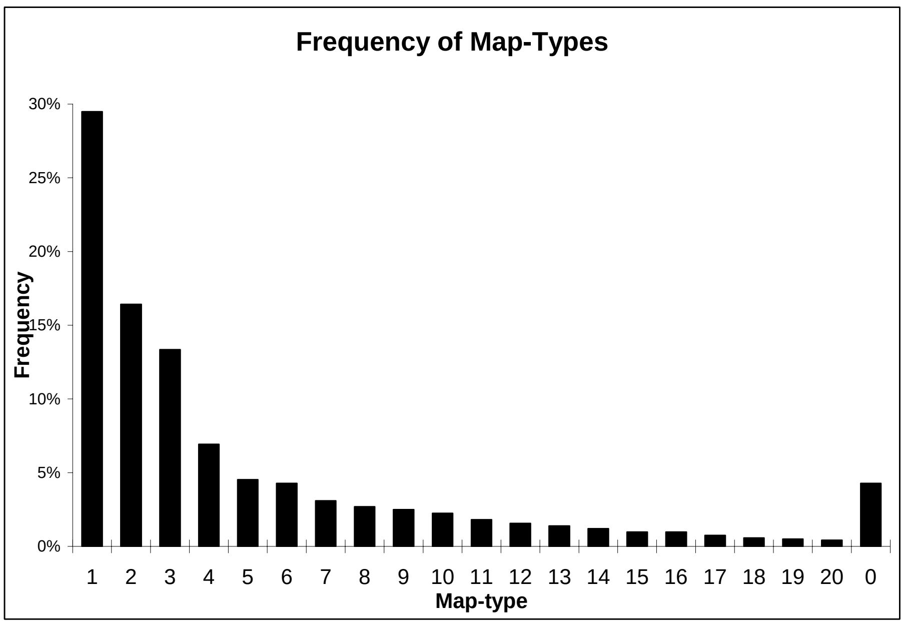

Figure 5.1: Frequency of map-types. Map-type ‘0’ is the unclassified group.

Map-type 1 is the most common map-type, occurring 30 percent of the time. This type is a mostly westerly flow pattern, but with a slight southwesterly push. A pattern close to this would result if all the days for the winter season were averaged together. Shown below is the key day representing map-type 1 along with the second and third highest correlated days in this map-type group. It can be seen that although the maps are not identical, their main flow pattern is very similar.

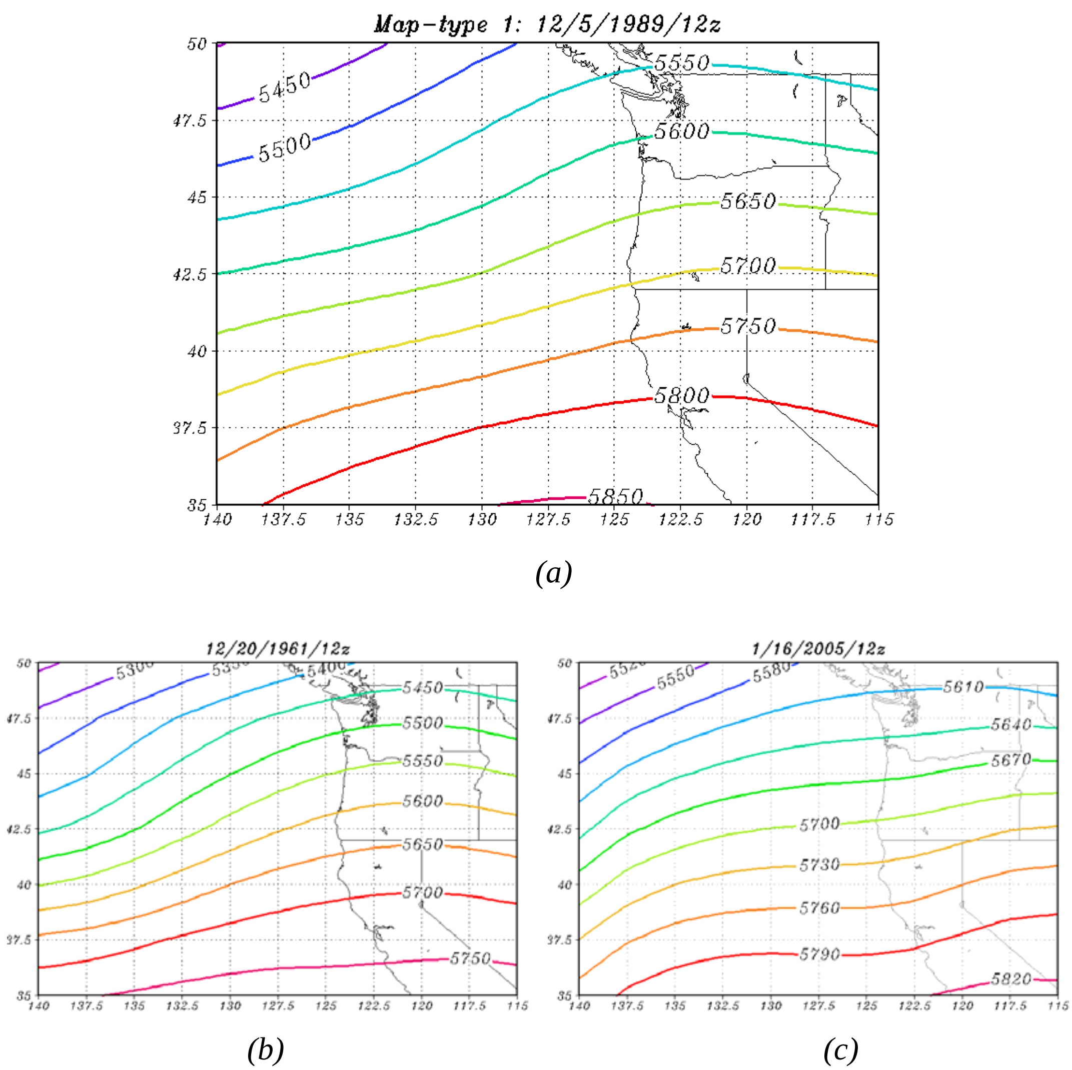

Figure 5.2: *(a)* Key day representing map-type 1. *(b)* Day with second highest correlation to map-type 1 *(c)* Day with third highest correlation to map-type 1.

Occurring 16% of the time, map-type 2 is the second most common map-type. This type is a northwesterly flow pattern. Maps found in this group have neither a strong ridge nor trough within the selected region affecting the flow.

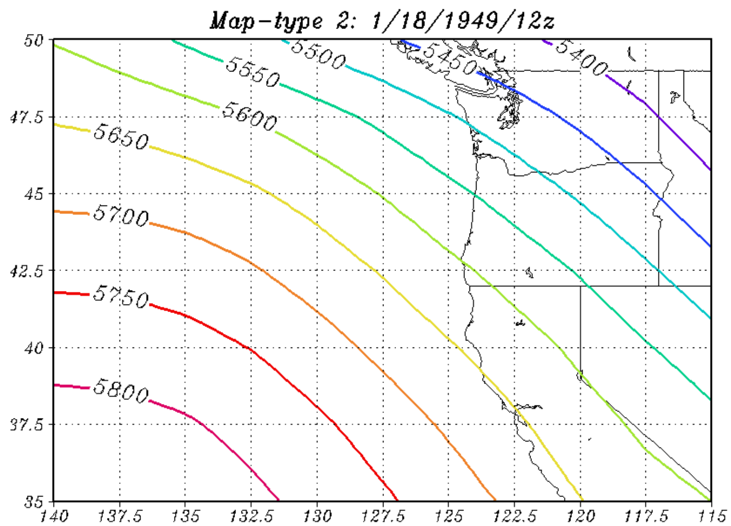

(a)

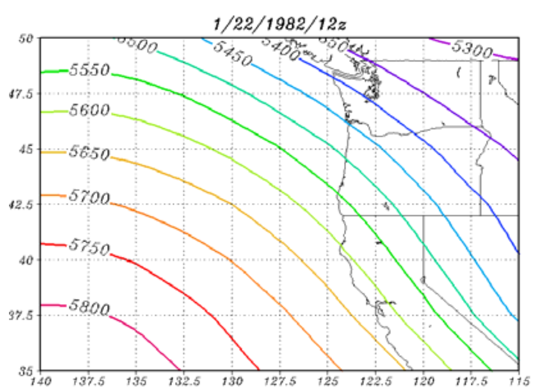

(b)

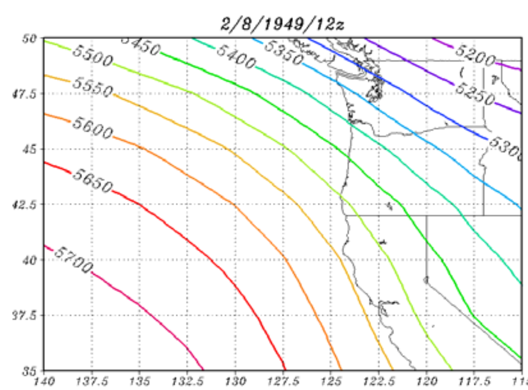

(c)

Figure 5.3: (a) Key day representing map-type 2. (b) Day with second highest correlation to map-type 2 (c) Day with third highest correlation to map-type 2.

Map-type 3 is the third most common map-type occurring 13% of the time. This type is a southwesterly flow pattern with a trough to the west of the selected region and a ridge to the east.

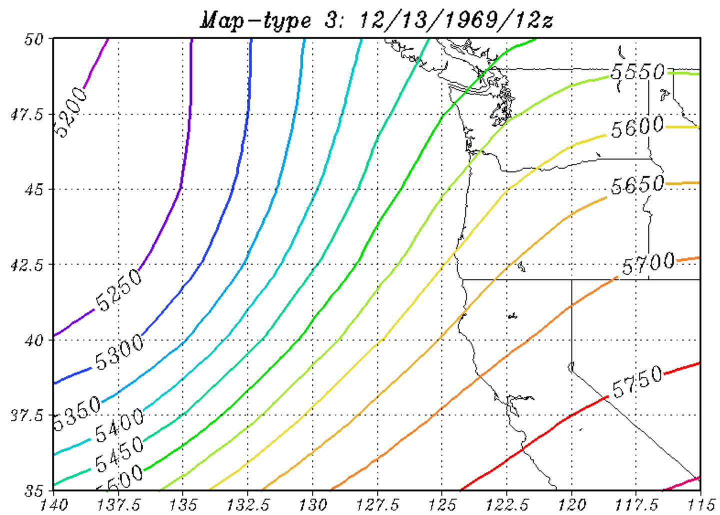

(a)

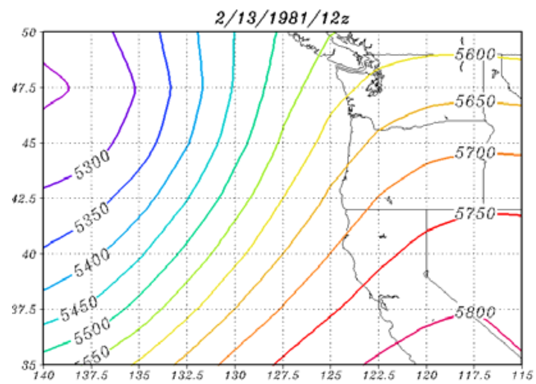

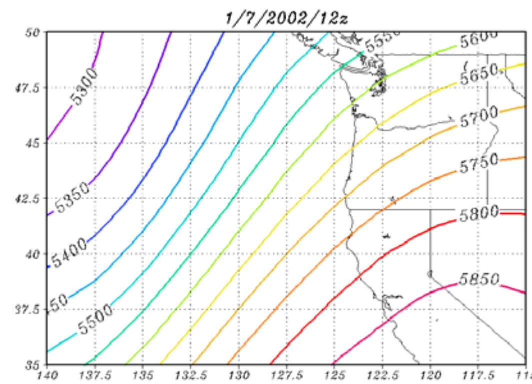

(b) *(c)*

Figure 5.4 : *(a)* Key day representing map-type 3. *(b)* Day with second highest correlation to map-type 3 *(c)* Day with third highest correlation to map-type 3.

Map-type 4 occurs 7% of the time. This type is distinguished by a slight trough in the center of the selected region, bringing northwesterly air in from the southwest.

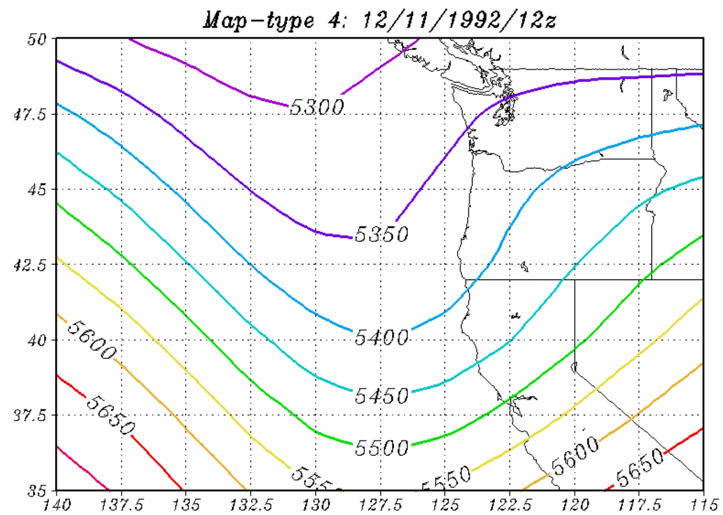

(a)

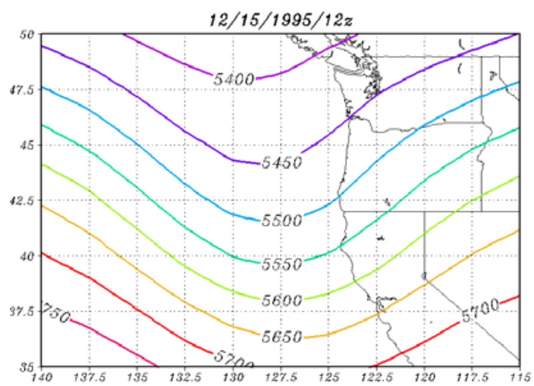

(b)

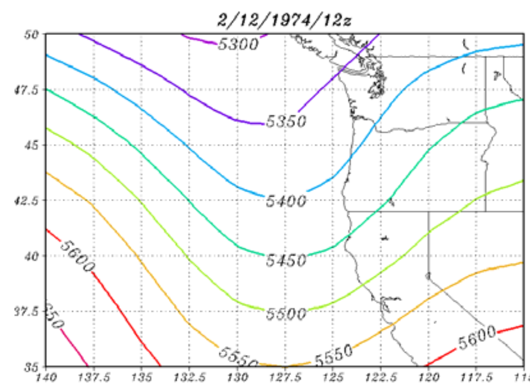

(c)

Figure 5.5: *(a)* Key day representing map-type 4. *(b)* Day with second highest correlation to map-type 4 *(c)* Day with third highest correlation to map-type 4.

Map-type 5 occurs 4.5% of the time. Maps found in this group have a strong ridge pulling air from the southwest in over the Gulf of Alaska, resulting in northerly flow over the Pacific Northwest.

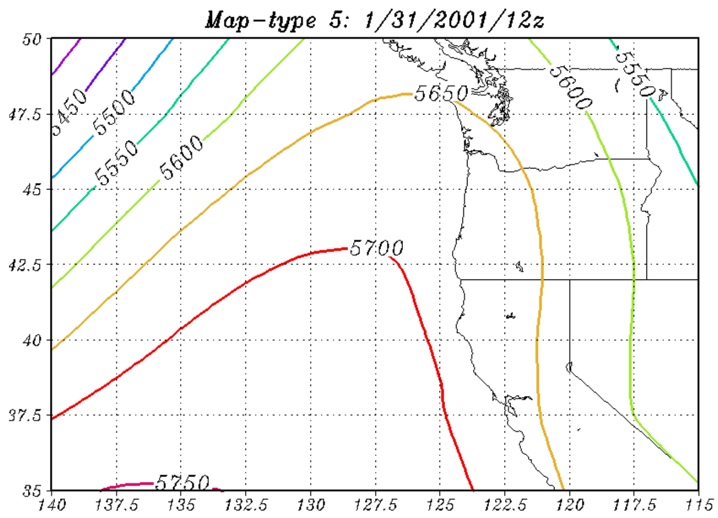

(a)

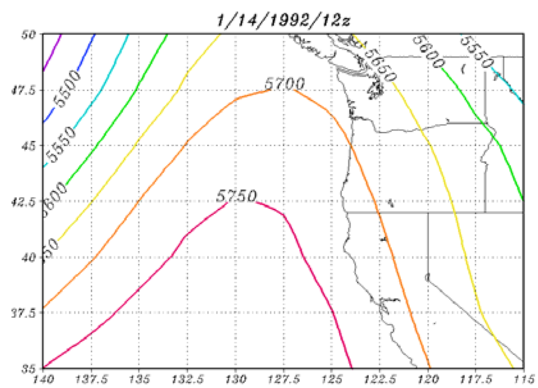

(b)

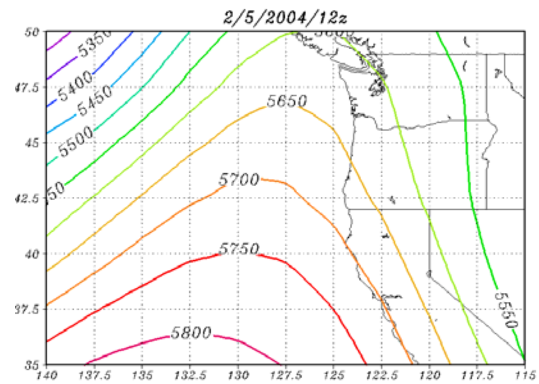

(c)

Figure 5.6: (a) Key day representing map-type 5. (b) Day with second highest correlation to map-type 5 (c) Day with third highest correlation to map-type 5.

Map-type 6 occurs just over 4% of time. This type has a similar shape to map-type 5 also bringing northerly flow over the Pacific Northwest. However, the ridge seen here is stronger, pushing air from the southwest further north.

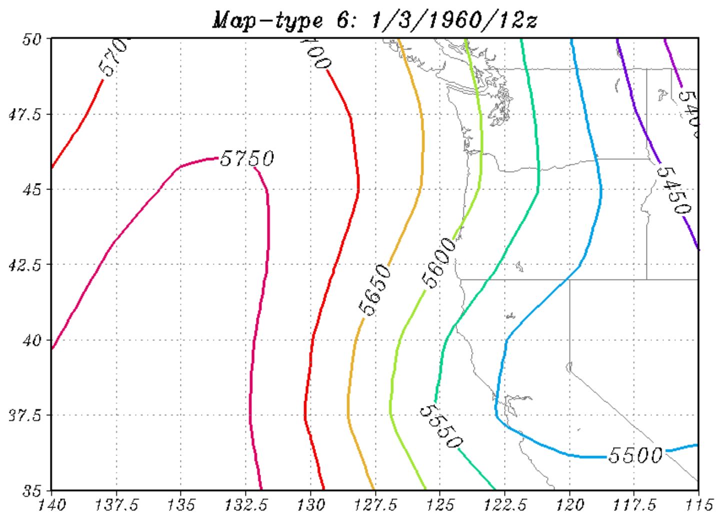

(a)

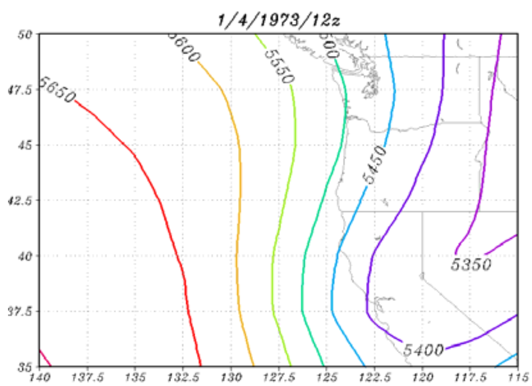

(b)

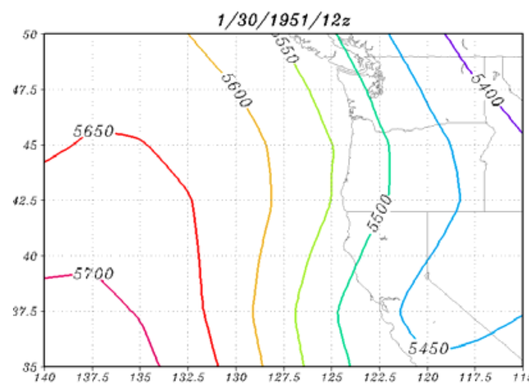

(c)

Figure 5.7: *(a)* Key day representing map-type 6. *(b)* Day with second highest correlation to map-type 6 *(c)* Day with third highest correlation to map-type 6.

Map-type 7 appears 3% of the time. This type is similar to five and six in that the main feature is a ridge; however, the ridge appearing in map-type 7 is much larger and further inland, centered over the northwest coast. A center of high pressure appears over northern California. Rather than resulting in northerly flow, this ridge brings a combination of southwesterly and northwesterly flow to the region, depending on the area of interest.

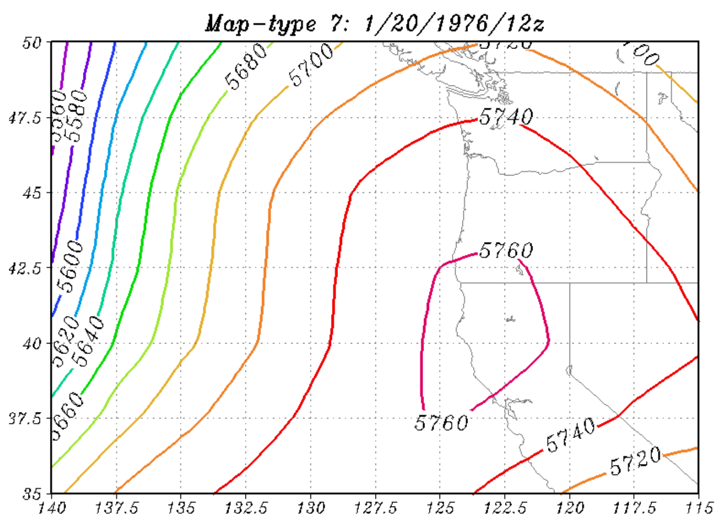

(a)

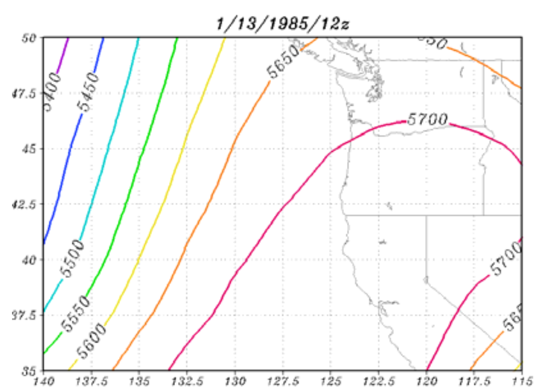

(b)

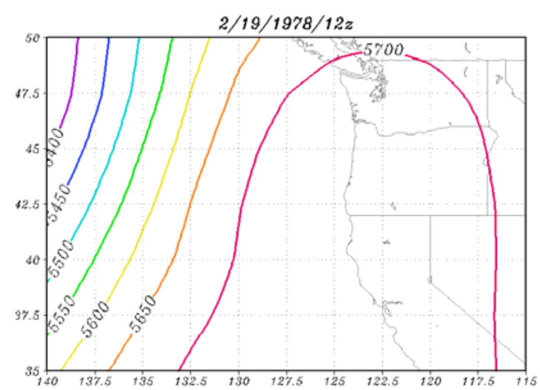

(c)

Figure 5.8: *(a)* Key day representing map-type 7. *(b)* Day with second highest correlation to map-type 7 *(c)* Day with third highest correlation to map-type 7.

Map-type 8 occurs just under three percent of the time. This map-type is distinguished by a deep trough that is centered over the Pacific Northwest. The flow enters the selected region from the northeast and is then rotated cyclonically within the selected region.

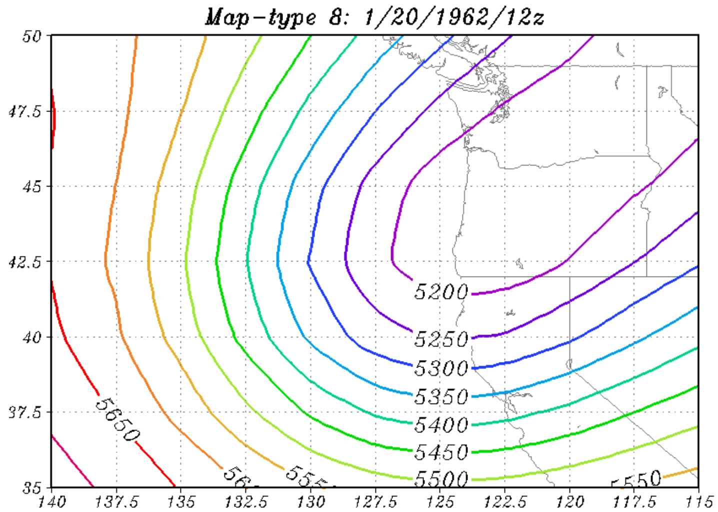

(a)

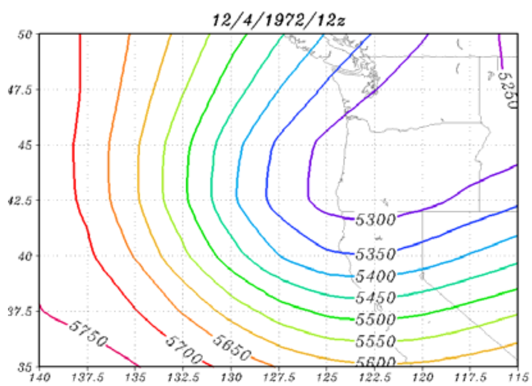

(b)

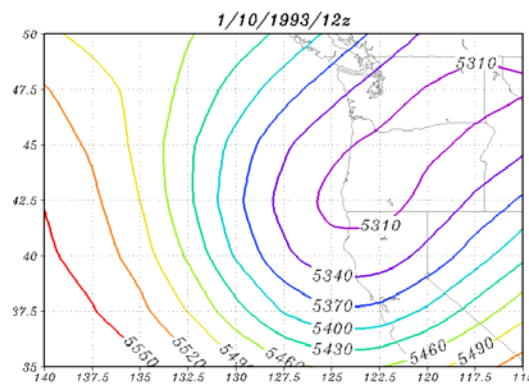

(c)

Figure 5.9: *(a)* Key day representing map-type 8. *(b)* Day with second highest correlation to map-type 8 *(c)* Day with third highest correlation to map-type 8.

Map-type 9 has a frequency of 2.5%. A deep trough appears on the west side of the selected region, resulting in southwesterly flow over the Pacific Northwest.

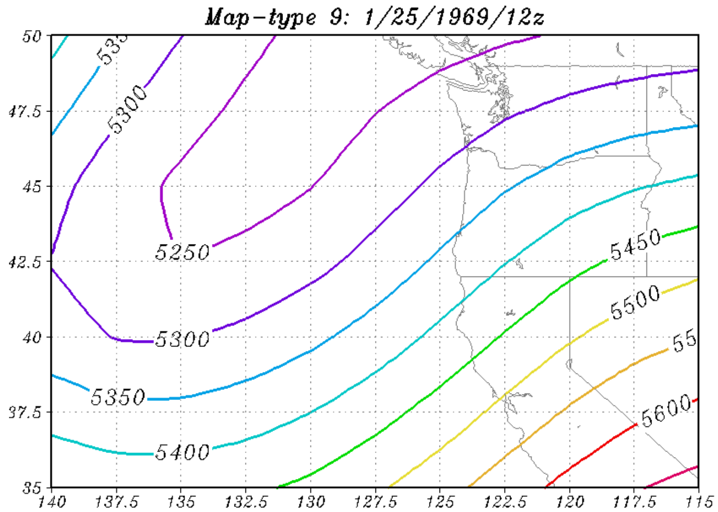

(a)

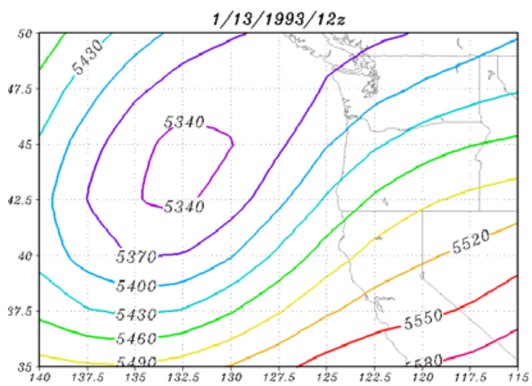

(b)

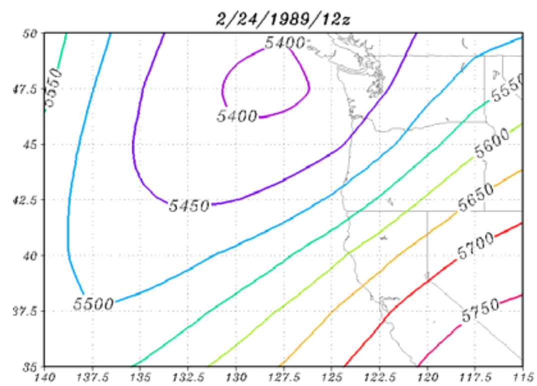

(c)

Figure 5.10: *(a)* Key day representing map-type 9. *(b)* Day with second highest correlation to map-type 9 *(c)* Day with third highest correlation to map-type 9.

Map-type 10 appears just over 2 percent of the time. Though ill defined in the western portion of the selected region, the flow is clearly north/northwesterly over the Pacific Northwest.

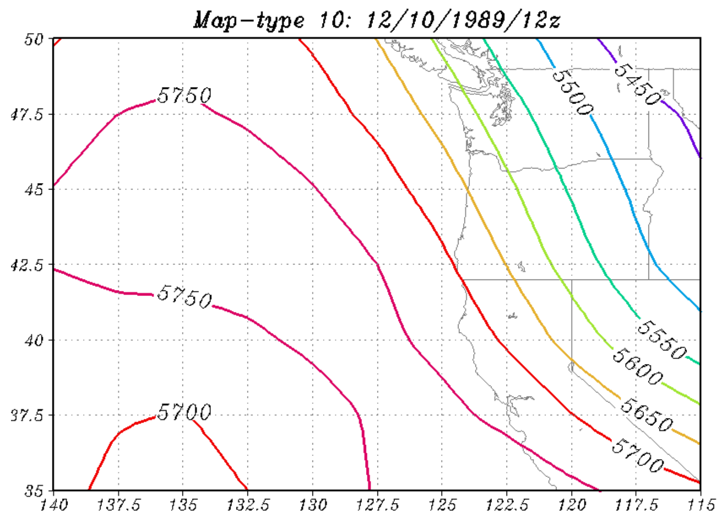

(a)

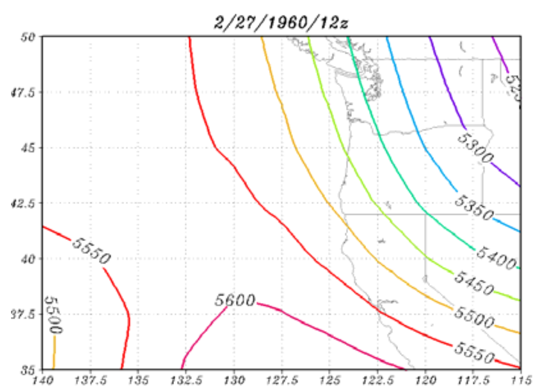

(b)

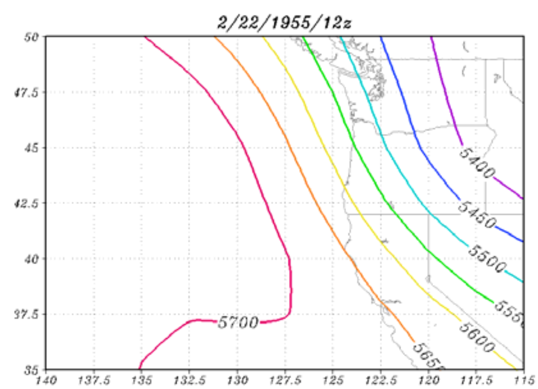

(c)

Figure 5.11: *(a)* Key day representing map-type 10. *(b)* Day with second highest correlation to map-type 10 *(c)* Day with third highest correlation to map-type 10.

Map-type 11 represents 1.8% of the maps classified. This type is similar to that of type 10, although the flow is more westerly than northerly.

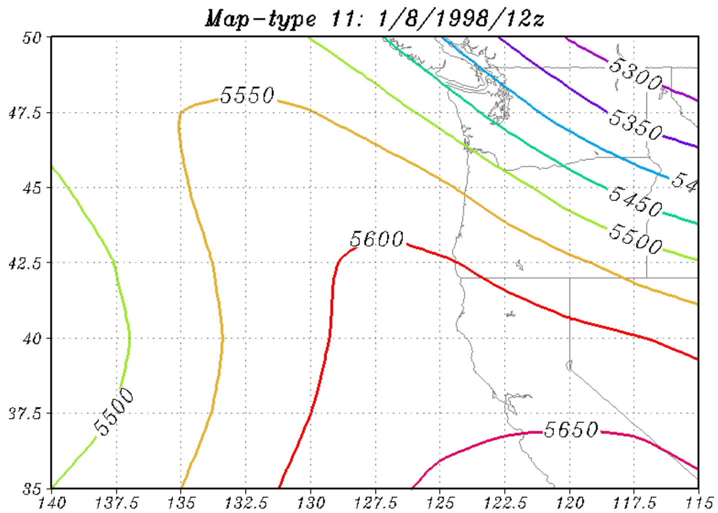

(a)

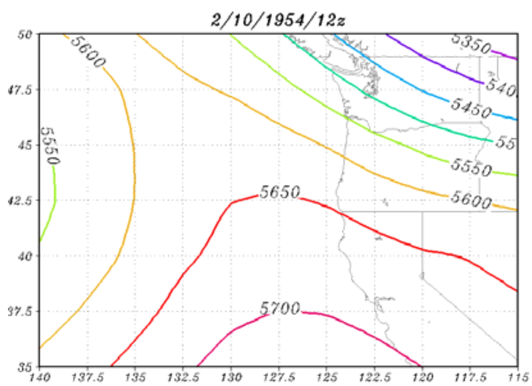

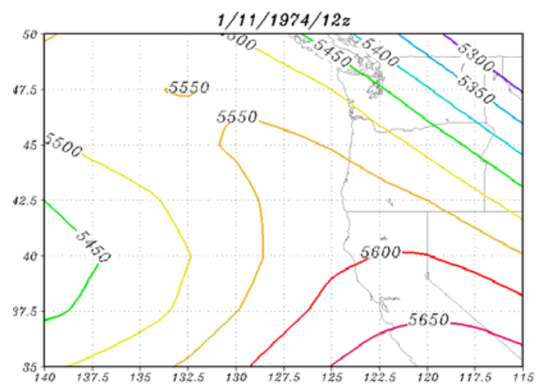

(b) (c)

Figure 5.12: (a) Key day representing map-type 11. (b) Day with second highest correlation to map-type 11 (c) Day with third highest correlation to map-type 11.

Map-type 12 occurs 1.6% of the time. Maps in this group each have a ridge off the coast, resulting in northerly flow over the Pacific Northwest.

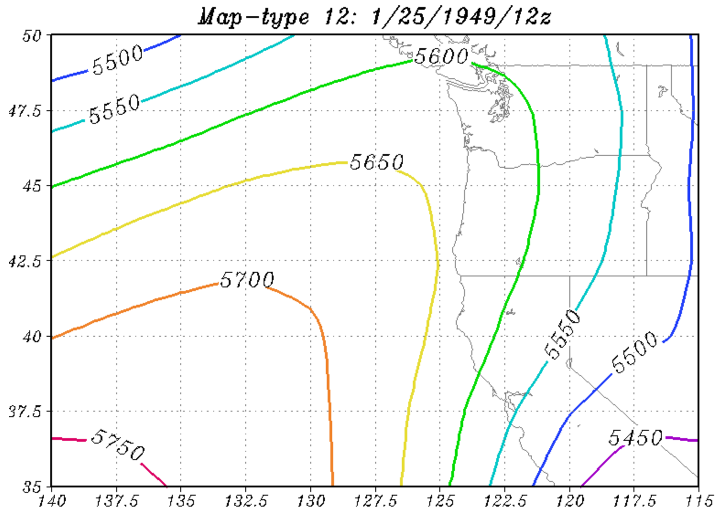

(a)

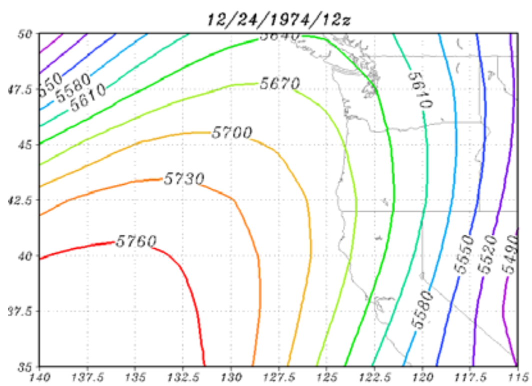

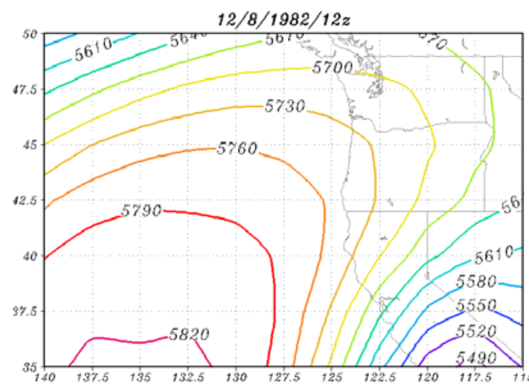

(b) *(c)*

Figure 5.13: *(a)* Key day representing map-type 12. *(b)* Day with second highest correlation to map-type 12 *(c)* Day with third highest correlation to map-type 12.

Map-type 13 occurs 1.4% of the time. Maps of this type are dominated by a mostly westerly flow pattern.

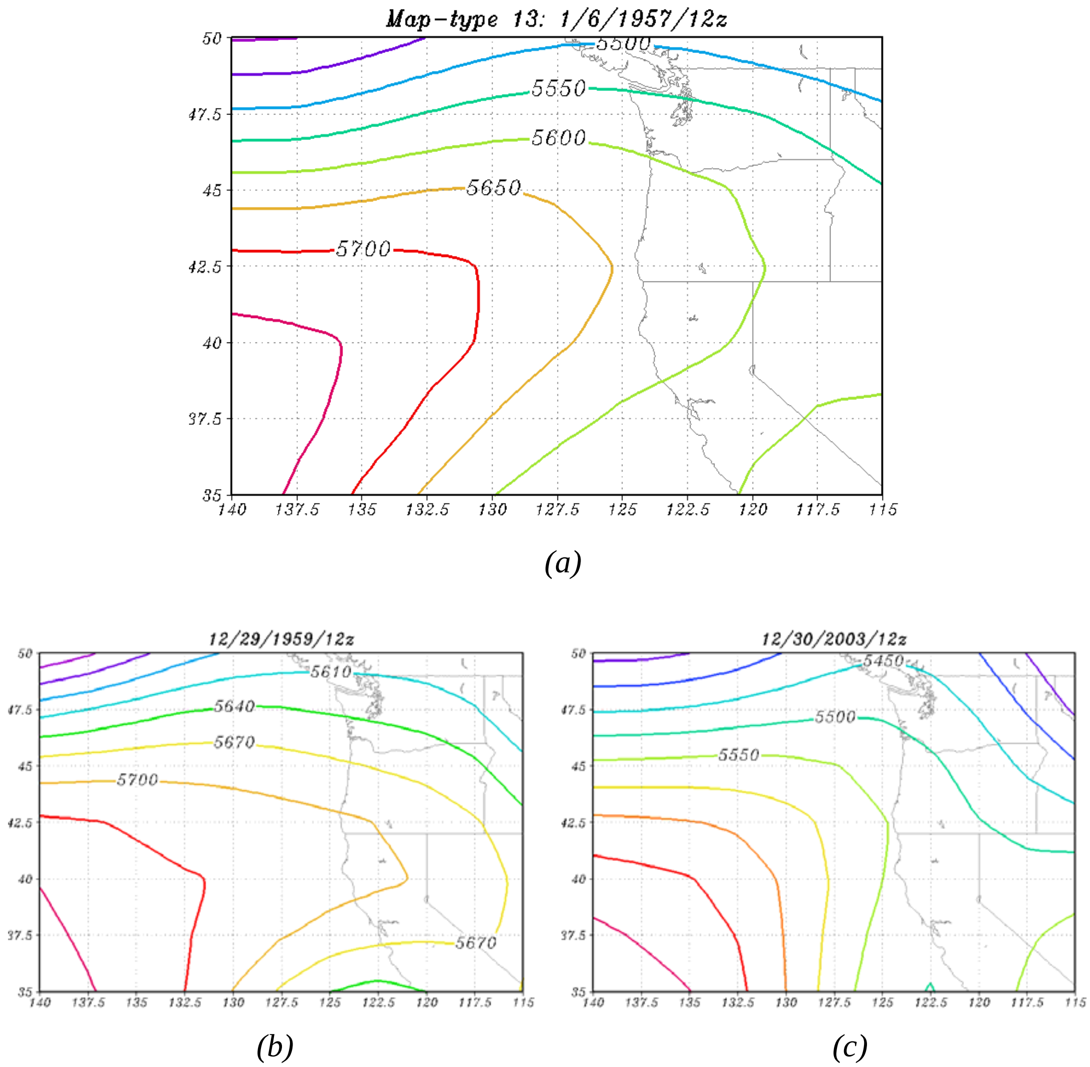

Figure 5.14: *(a)* Key day representing map-type 13. *(b)* Day with second highest correlation to map-type 13 *(c)* Day with third highest correlation to map-type 13.

Map-type 14 occurs 1.2% of the time. For the area selected, it is difficult to define the flow for this map-type. The flow is split off the coast of Oregon, resulting in a mostly southerly flow over the Pacific Northwest.

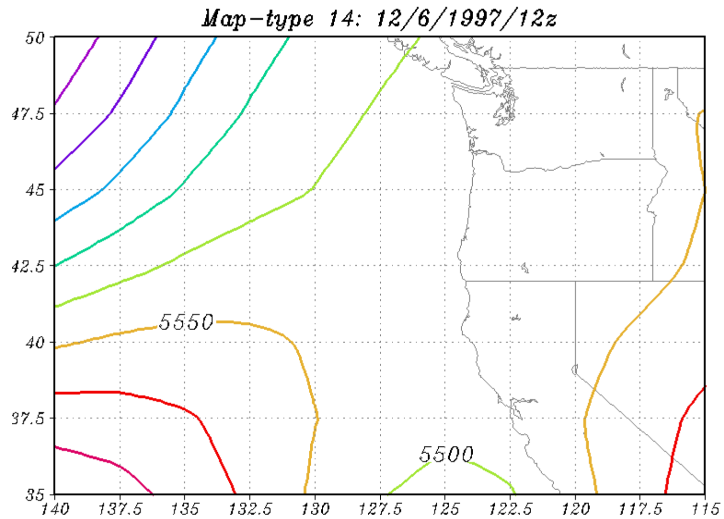

(a)

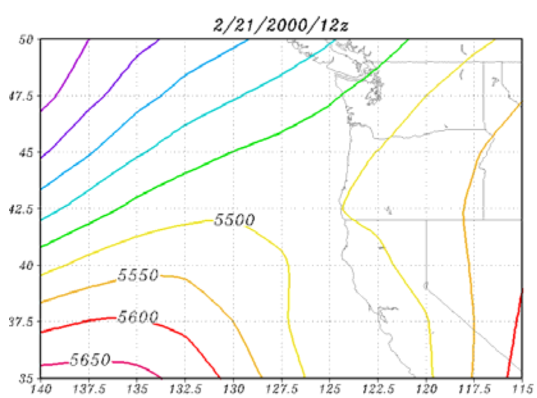

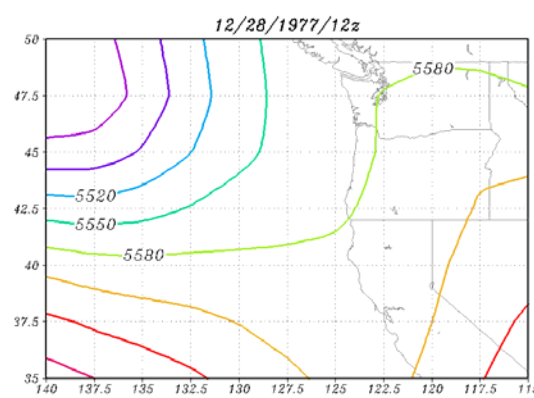

(b) *(c)*

Figure 5.15: *(a)* Key day representing map-type 14. *(b)* Day with second highest correlation to map-type 14 *(c)* Day with third highest correlation to map-type 14.

Map-type 15 occurs 1% of the time. This map-type is dominated by a region of low pressure off the in the southwest corner of the selected region. The resulting flow over land is mostly southerly as it is being influenced by the cyclonic rotation around the low-pressure center.

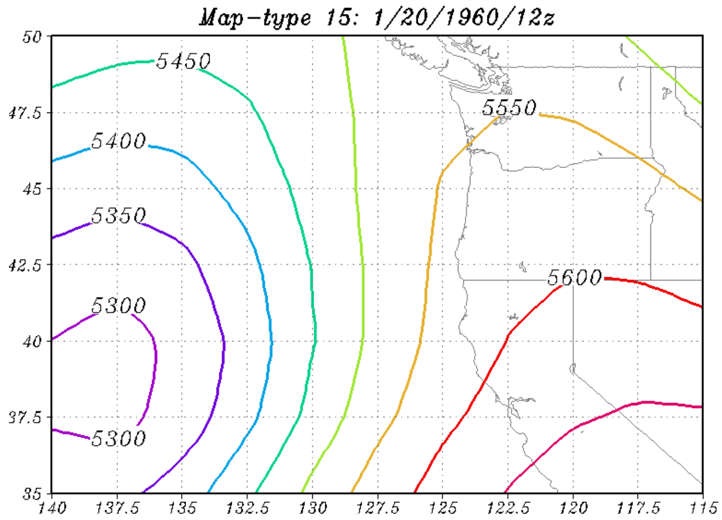

(a)

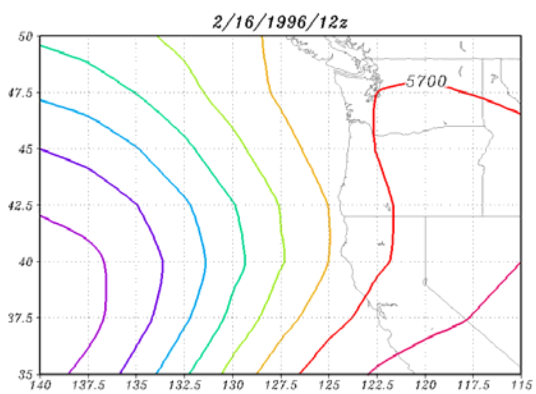

(b)

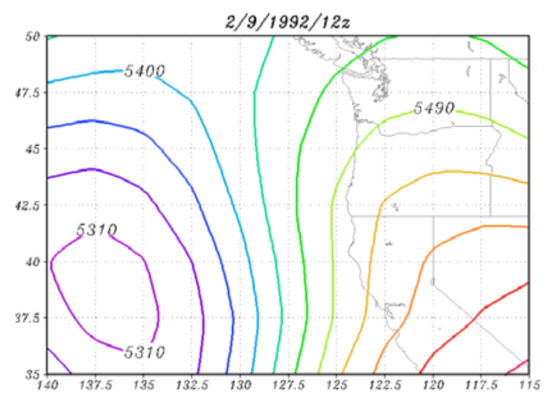

(c)

Figure 5.16: *(a)* Key day representing map-type 15. *(b)* Day with second highest correlation to map-type 15 *(c)* Day with third highest correlation to map-type 15.

Map-type 16 occurs 1% of the time. Maps in this type are similar to type 15 maps in that there is a low-pressure center in the selected area. Although, the low pressure center seen here is further inland, causing the flow to come more directly from the south rather than the southwest.

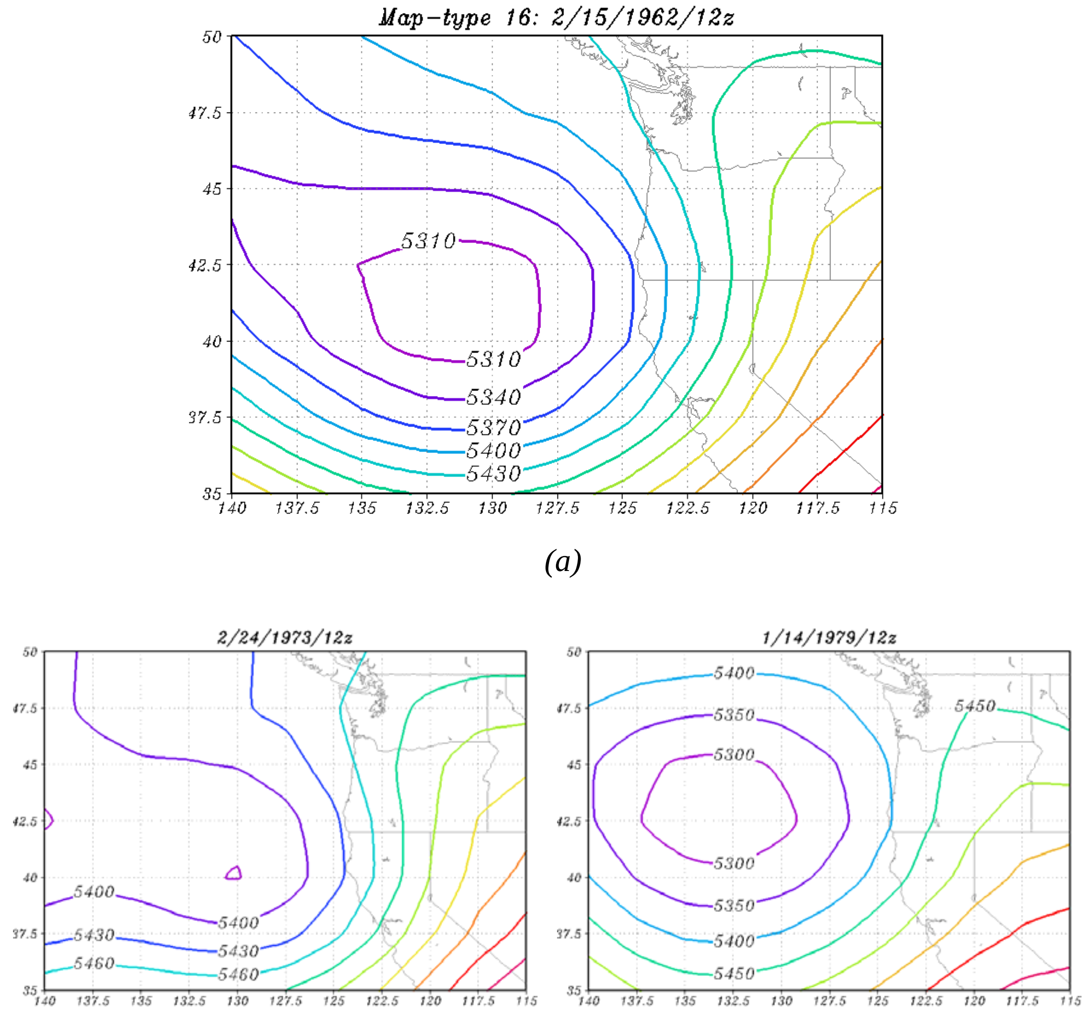

Figure 5.17: *(a)* Key day representing map-type 16. *(b)* Day with second highest correlation to map-type 16 *(c)* Day with third highest correlation to map-type 16.

Map-type 17 occurs 0.7 % of the time. Maps in this group contain a high ridge centered over Washington along with a trough to the west. This creates a flow pattern that is from the southeast. Map-type 17 is the only group with a southeasterly flow pattern.

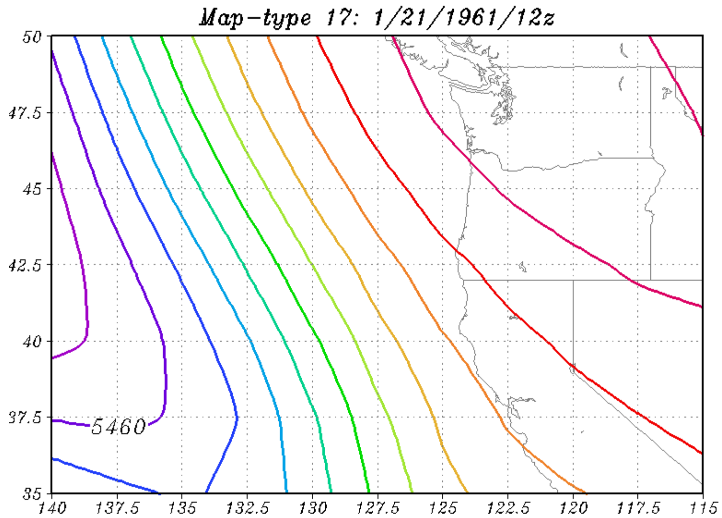

(a)

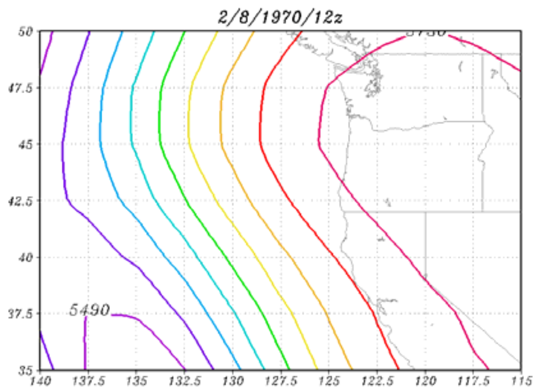

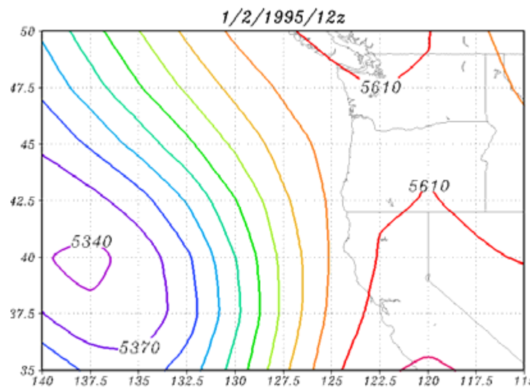

(b) *(c)*

Figure 5.18: *(a)* Key day representing map-type 17. *(b)* Day with second highest correlation to map-type 17 *(c)* Day with third highest correlation to map-type 17.

Map-type 18 occurs 0.6% of the time. The distinct feature of this group is the large area of high pressure centered along the coast of southern Oregon. The resulting flow over the Pacific Northwest is from the northwest.

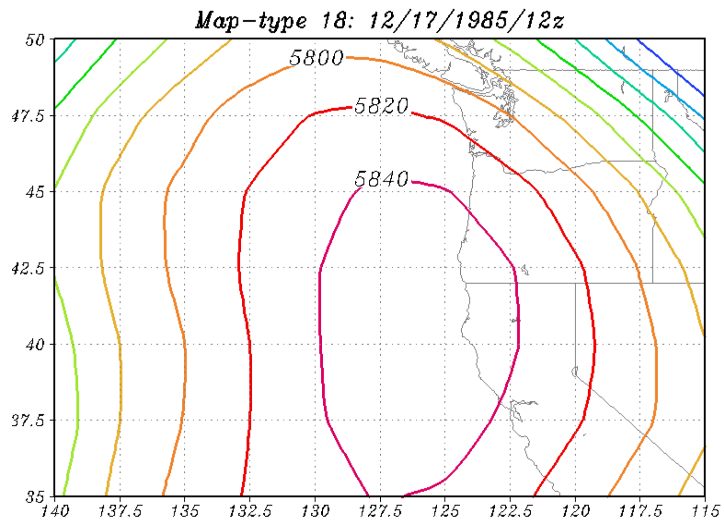

(a)

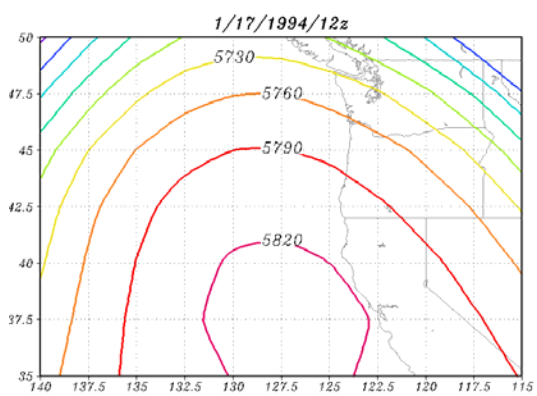

(b)

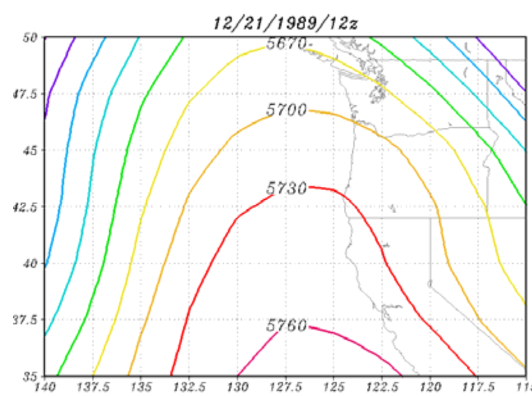

(c)

Figure 5.19: *(a)* Key day representing map-type 18. *(b)* Day with second highest correlation to map-type 18 *(c)* Day with third highest correlation to map-type 18.

Map-type 19 occurs 0.5 % of the time. A feature seen with type 19 maps is an area of low pressure centered over southern California. The resulting flow over the Pacific Northwest is northeasterly.

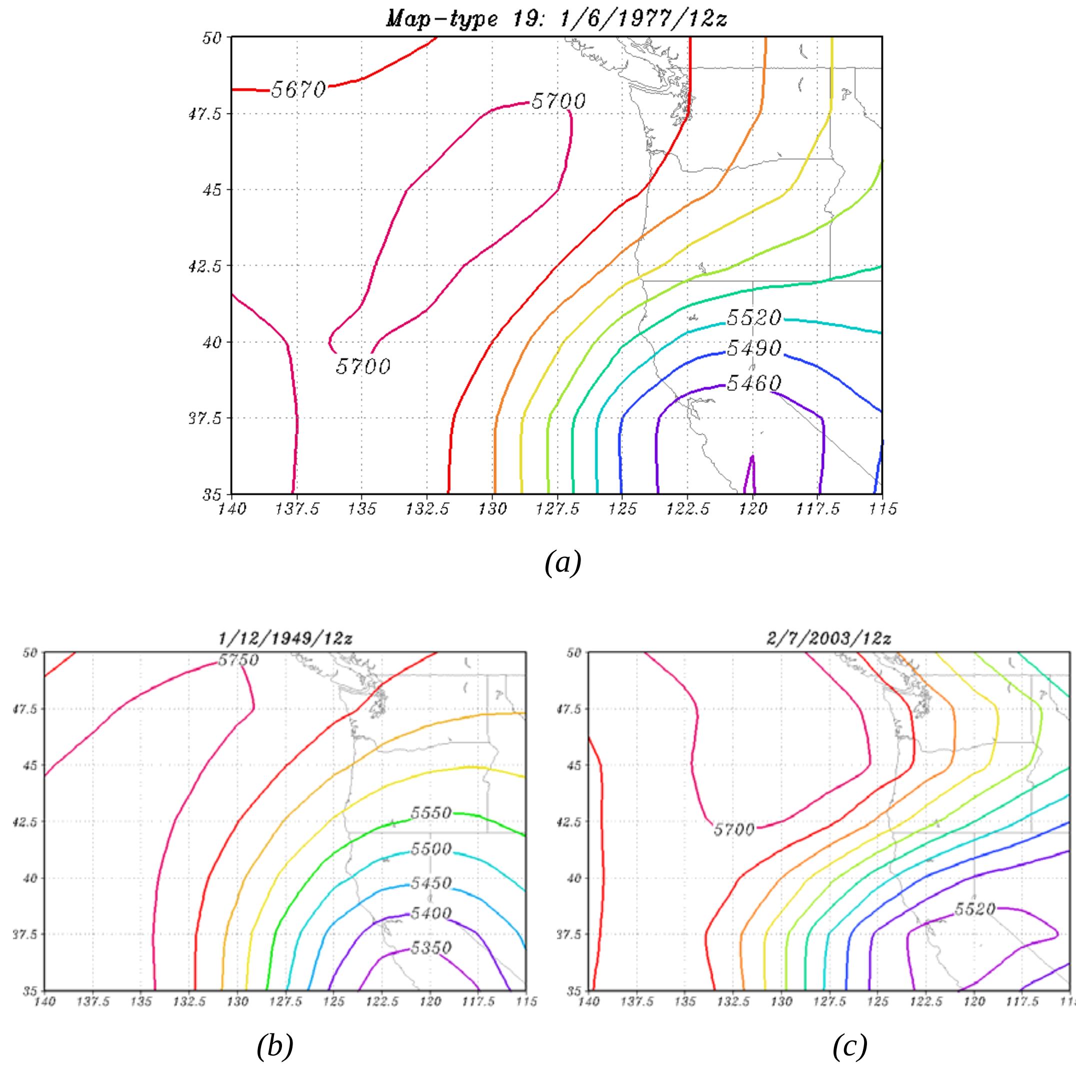

Figure 5.20: *(a)* Key day representing map-type 19. *(b)* Day with second highest correlation to map-type 19 *(c)* Day with third highest correlation to map-type 19.

Map-type 20 occurs 0.4 % of the time. This group of maps is influenced by two low-pressure areas, one to the northeast and one to the south. The flow direction depends on the area of interest.

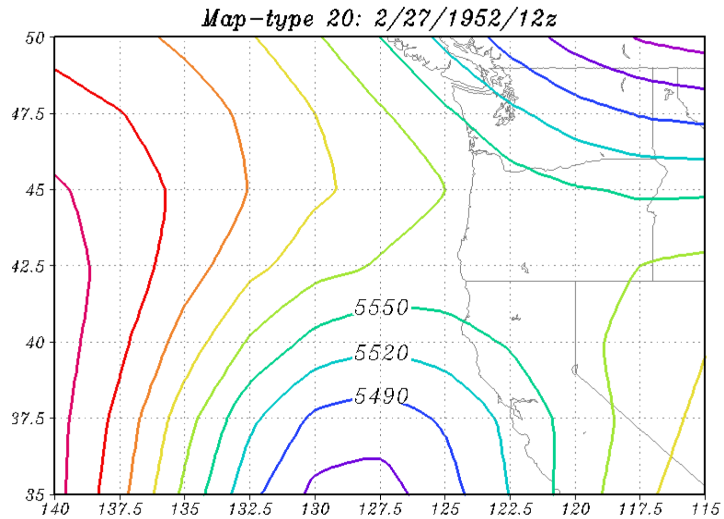

(a)

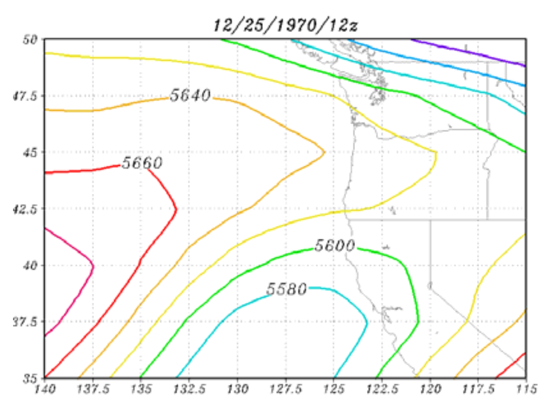

(b)

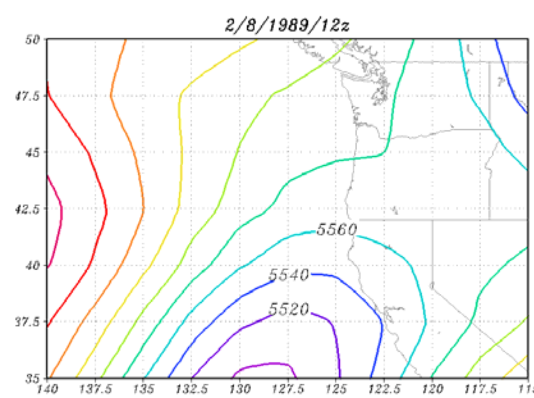

(c)

Figure 5.21: *(a)* Key day representing map-type 20 *(b)* Day with second highest correlation to map-type 20 *(c)* Day with third highest correlation to map-type 20.

This collection of map-types provides a catalog of the main flow patterns that occur over the Pacific Northwest, each with a distinct pattern. In order to better understand the weather that occurs over the Pacific Northwest, these map-types must be correlated with weather data from the surface, which is the second step in creating a synoptic map-type climatology.

6 Comparing the Surface Environment to Synoptic Map-Types

Weather at the surface is closely related to the flow patterns that are occurring aloft. The second step of this study is to create an objective record of weather that results from each map-type by correlating map-types with surface weather data. Four variables were chosen to accomplish this: daily maximum temperature, daily minimum temperature, daily precipitation totals, and daily snowfall totals. Other weather variables could readily be added in future studies.

In order to obtain a thorough understanding of the relationship between the flow at 500 millibars and the surface environment, each of the four variables was analyzed over a wide range of spatial scales, stretching from a single city to an average of the entire Pacific Northwest. Record events for each variable were also correlated with the map-typing data to explore any correlations between map-type and extreme weather events. Furthermore, this study explored relationships between ENSO (El Niño or La Niña years) and map-type.

The data used to calculate the "Pacific Northwest Average" were taken from 22 stations throughout Oregon and Washington (see figure 6.22). The stations were chosen based on location to ensure the data were representative of the entire state. The quality and quantity of historical data available were considered when choosing stations to represent each area of the Pacific Northwest. Corvallis was chosen as the individual city to research given the quantity and reliability of its data. Both the

Corvallis data and the Oregon climate zone data were provided by the Oregon Climate Service.

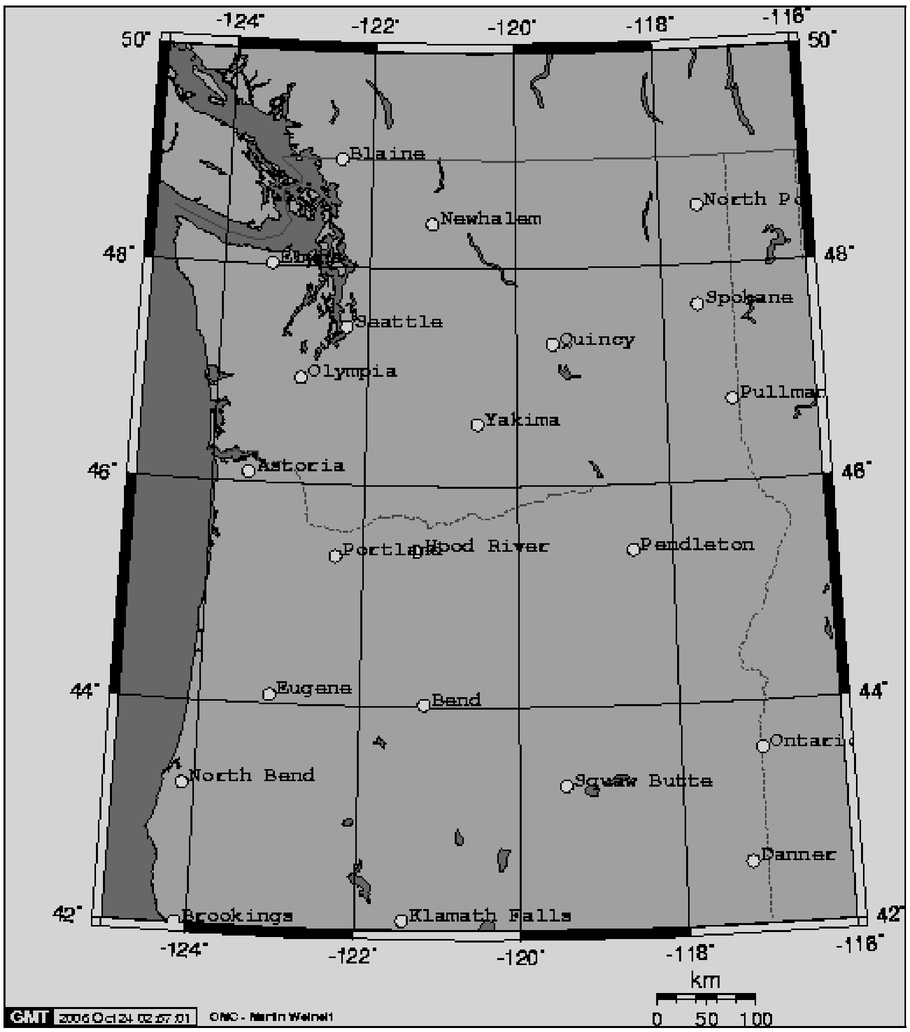

Figure 6.1: Map of stations used for calculating “Pacific Northwest Average”.

The following results are displayed first by variable then by area of interest. Each data set covers the same record used for the map-typing study, which are the winter months of 1948-2005.

6.1 Maximum Temperature

6.1.1 NW Regional Averages

When correlating map-type and average maximum temperature across Oregon and Washington, the first step is to separate all of the historical daily maximum temperatures for each of the 22 stations by the map-type chosen for each date. Once grouped by map-type, a mean temperature is calculated for the Northwest as a whole. Figure 6.2 shows the daily maximum temperature for each map-type group, including the mean, maximum, minimum and standard deviation values.

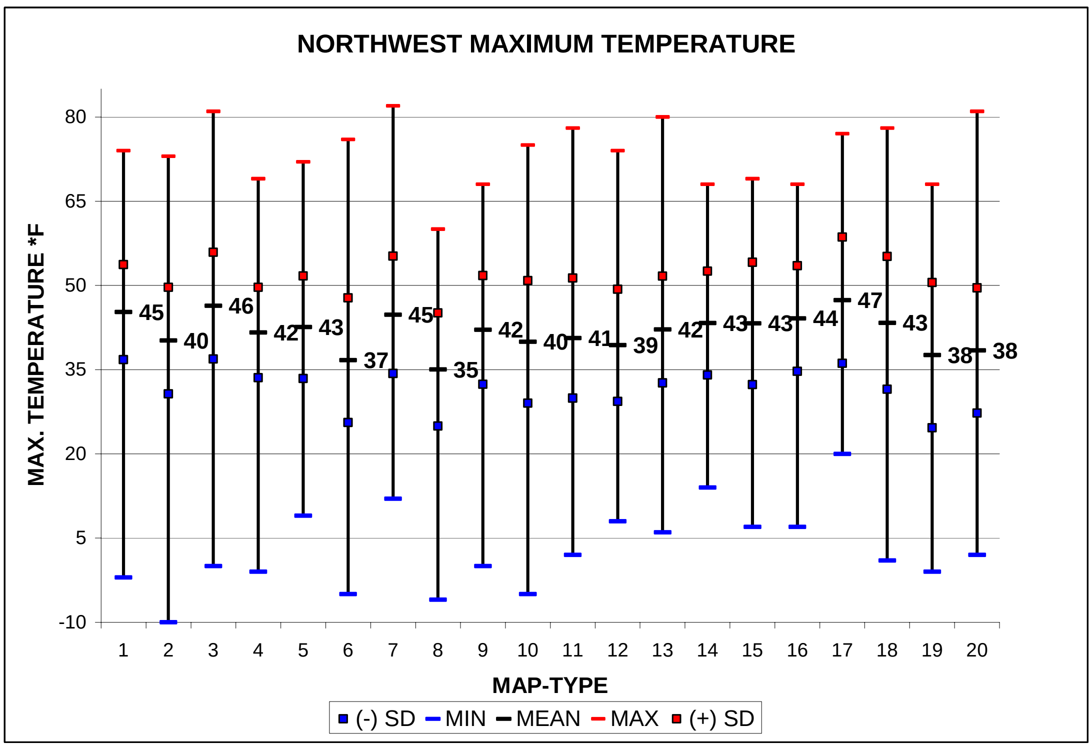

Figure 6.2: Average daily maximum temperature in degrees Fahrenheit by map-type, showing the mean, maximum, minimum, and standard deviation values.

Table 6-1: Corresponding values for Figure 6.2, showing the mean, standard deviation, minimum and maximum values for daily maximum temperature by map-type for the Pacific Northwest average.

	1	2	3	4	5	6	7	8	9	10	11	12	13	14	15	16	17	18	19	20
MEAN	45	40	46	42	43	37	45	35	42	40	41	39	42	43	43	44	47	43	38	38
SD	8	9	10	8	9	11	10	10	10	11	11	10	10	9	11	9	11	12	13	11
MIN	-2	-10	0	-1	9	-5	12	-6	0	-5	2	8	6	14	7	7	20	1	-1	2
MAX	74	73	81	69	72	76	82	60	68	75	78	74	80	68	69	68	77	78	68	81

When looking at figure 6.2 and table 6-1, it is quickly seen that the warmest map-type on average is 17 and the coldest map-type is eight. These two map-types result in a difference of over 12 °F on average. Referring back to the descriptions of the map-types in Chapter 5, type 17 is the only map-type with flow from the southeast; it includes a ridge of high pressure, where as map-type 8 consists of flow from the northeast around a deep trough of low pressure (see figure 6.3 a and b). These two relationships are an example of how an objective synoptic climatology provides statistical information about the relationship between flow aloft and the surface environment.

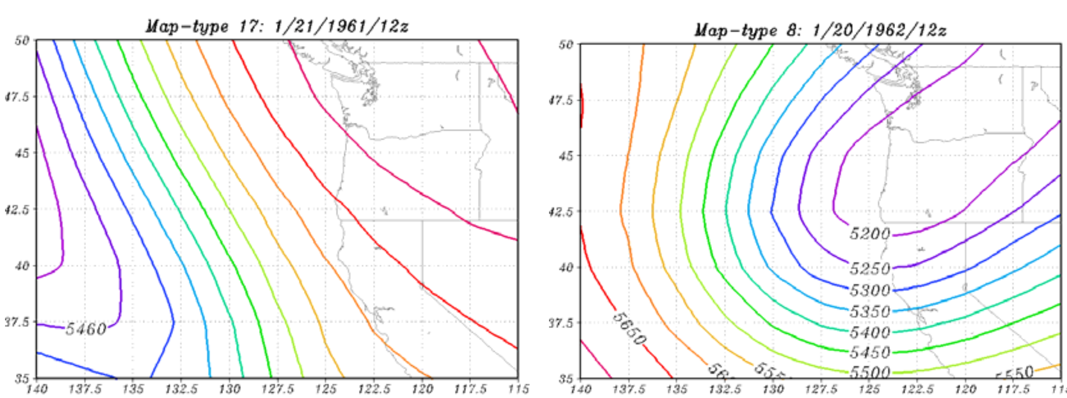

(a) (b)

Figure 6.3: *(a)* Map-type 17-the warmest map-type for the Pacific Northwest average. *(b)* Map-type 8-the coldest map-type for the Pacific Northwest average.

6.1.2 Average by Oregon Climate Zones

The state of Oregon is divided into nine zones by climate type (see figure 6.4). Zones 1,2,6,7 and 9 were chosen for this study based on the quantity and quality of data available from stations in these five zones. The stations located in each zone are shown in Table 6-2.

Table 6-2: Lists the stations located in each zone that were used to calculate the "Zone Averages".

	Zone 1	Zone 2	Zone 6	Zone 7	Zone 9
Stations	Astoria	Eugene	Hood River	Bend	Ontario
	Brookings	Portland	Pendleton	Klamath Falls	Danner
	North Bend			Squaw Butte	

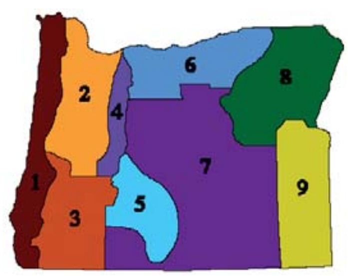

Figure 6.4: Oregon climate zones

The average daily maximum temperature for each of the Oregon climate zones was calculated similarly to how the northwest average was calculated. First each of the 5,235 days in the data set was categorized by map-type, then the daily maximum temperature from the stations in each zone were averaged together to find the average maximum temperature for each map-type in each zone. The zone data includes a much smaller region then the entire Northwest data and therefore each zone may be influenced by a different part of the atmospheric flow. Figure 6.5 presents the average maximum temperature for each zone. Table 6-3 lists the coldest map-type and warmest map-type for each zone.

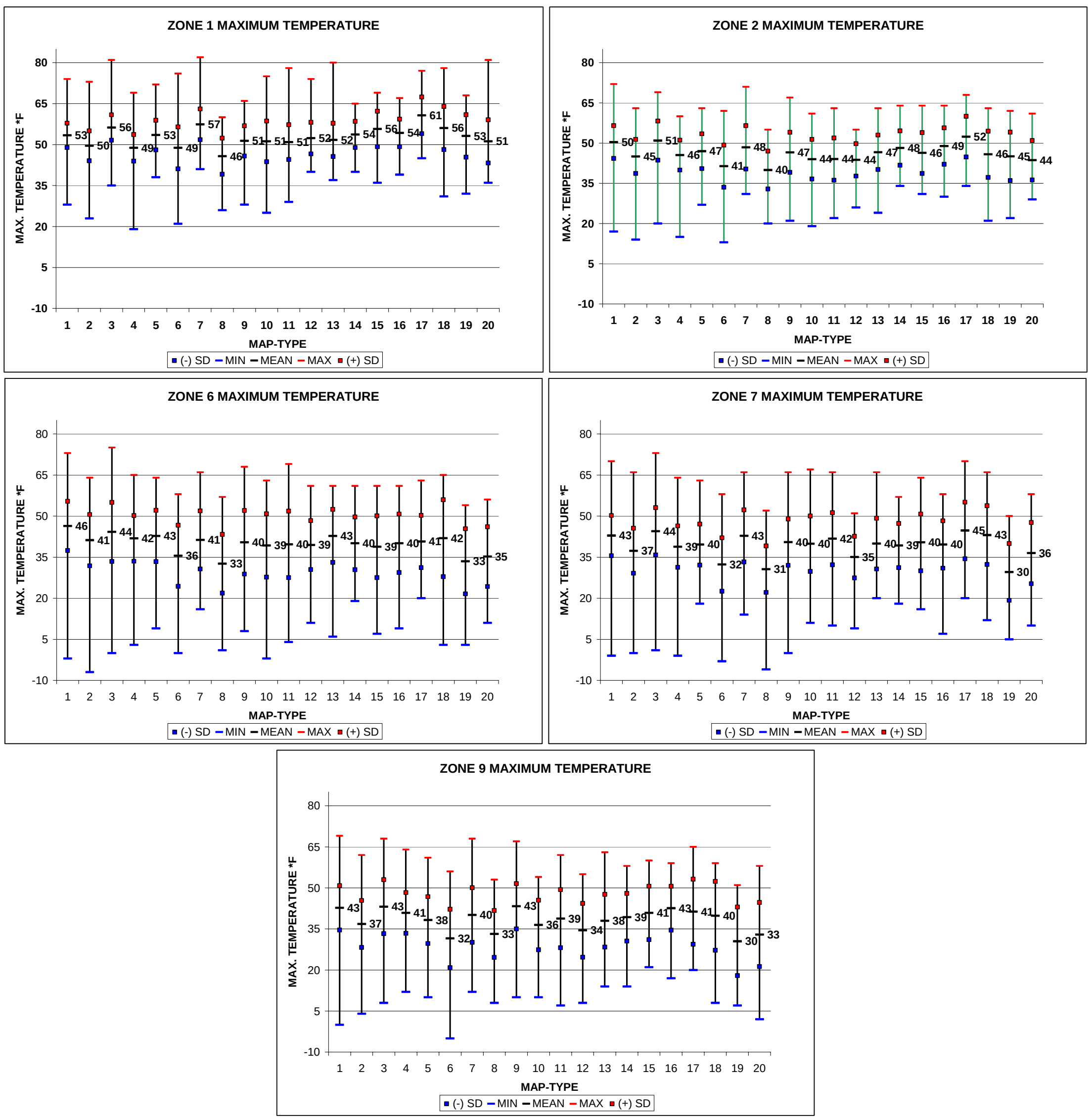

Figure 6.5: Maximum temperature for each map-type for climate zones 1, 2, 6, 7 and 9, showing the mean, standard deviation, maximum, and minimum values.

Table 6-3: Average warmest map-type and average coldest map-type for each zone.

	Coldest Map-Type	Warmest Map-Type
NW	8	17
Zone 1	8	17
Zone 2	8	17
Zone 6	8	1
Zone 7	19	17
Zone 9	19	9

Table 6-3 shows that zones 1 and 2 have the same warmest and coldest map-type as the Northwest regional average. However, zones 6 and 9 have a different warmest map-type and zones 7 and 9 have a different coldest map-type. This analysis demonstrates that each climate zone may be influenced by a different part of the flow than that which affects the whole Oregon and Washington region. The following section looks at the smallest area of study.

6.1.3 Corvallis Averages

Data from the single city of Corvallis, Oregon was chosen as the smallest spatial scale to analyze. Data was available for each of the four variables for the entire 58-year period. This analysis was conducted in the same way as was done for the northwest average and the Oregon climate zone data.

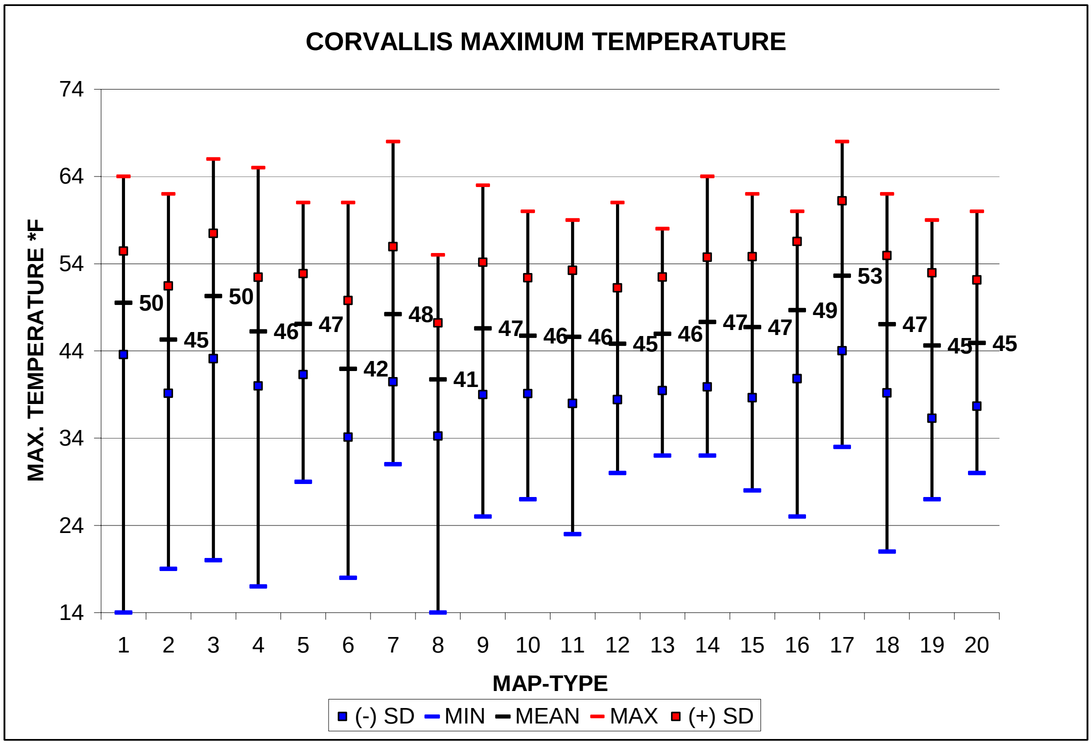

Figure 6.6: Daily maximum temperature in Corvallis, Oregon by map-type, including the mean, standard deviations, maximum and minimum values.

Table 6-4: Corresponding values for Figure 6.6, showing the mean, standard deviation, minimum and maximum values for daily maximum temperature by map-type for Corvallis.

	1	2	3	4	5	6	7	8	9	10	11	12	13	14	15	16	17	18	19	20
MEAN	50	45	50	46	47	42	48	41	47	46	46	45	46	47	47	49	53	47	45	45
SD	6	6.2	7	6	6	8	8	6	8	6.6	8	6	7	7	8	8	9	8	8	7
MIN	14	19	20	17	29	18	31	14	25	27	23	30	32	32	28	25	33	21	27	30
MAX	64	62	66	65	61	61	68	55	63	60	59	61	58	64	62	60	68	62	59	60

Figure 6.6 and Table 6-4 show the average maximum temperature in Corvallis, Oregon for each map-type. As was seen for the northwest average and zones 1, 2, and 7, map-type 17 is the warmest type in Corvallis as well. The coldest map-type for

Corvallis is type 8, which is also the coldest for the northwest average and for zones 1, 2 and 6.

6.1.4 Corvallis Record Events

Extreme weather events are often a concern to weather forecasters. To calculate the chance of a record maximum temperature, each of the 91 current record dates for the three winter months were categorized by map-type. If the record for any given date occurred prior to 1948, that day's record was not included and if there was a tie, both dates were included. The results shown in figure 6.7 were normalized by dividing the number of record events in each map-type by the total number of days in that map-type.

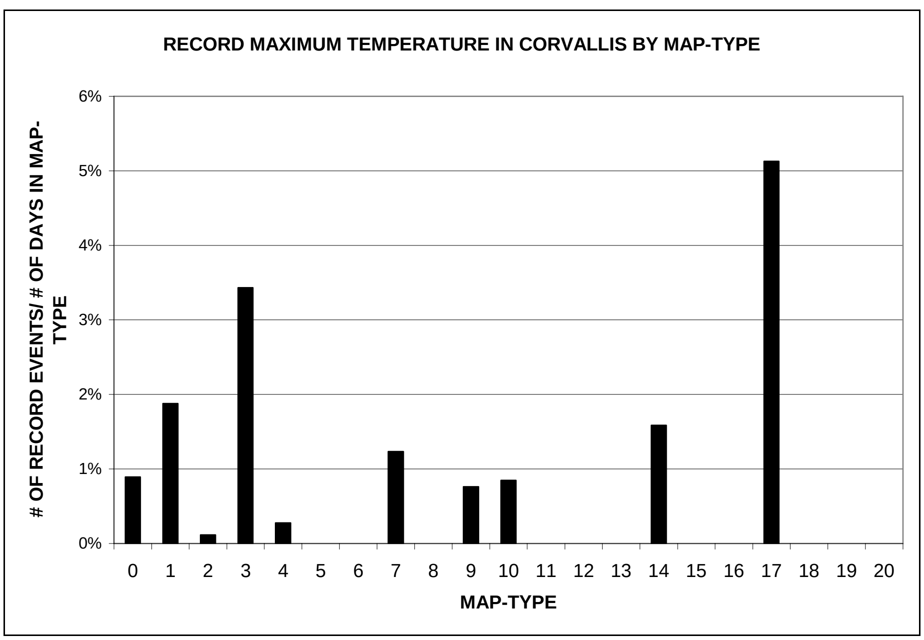

Figure 6.7: Normalized frequency of Record Maximum Temperature in Corvallis, Oregon by map-type, calculated by taking the # of record events in each map-type/ the number of days in each map-type. Only records that occurred after 1948 were included in the study.

When comparing map-type to record maximum temperatures in Corvallis, it is seen that map-type 17 has the greatest chance of setting a record high temperature for any given winter day. Additionally, the top five record producing map-types are also the warmest or second warmest map-type for the Northwest, all five climate zones and Corvallis. Of equal importance is the result that none of the days classified into map-types 5, 6, 8, 11, 12, 13, 15, 16, 18, 19 and 20 currently hold a record high temperature in Corvallis during the months of December, January and February.

6.1.5 Spatial Scale Comparison and the Departure from the Mean

For each distinct flow type there was a distinct correlation to maximum temperature. Additionally, researching the connection between map-type and record maximum temperature demonstrated the strong influence of southeasterly and northeasterly flow on the Pacific Northwest and the distinction between warmer and colder flow patterns. Figure 6.8 shows the departure from the mean average maximum temperature for each map-type for all of the spatial scales analyzed. This chart reveals which map-types are typically colder than average and which are typically warmer than average. Additionally it can be seen which map-types are associated with maximum temperatures that are closer to the normal, as opposed to those that are associated with extremes. Map-types 1, 2, 3, 6, 8, 10, 12 and 20 are always warmer or colder than average, regardless of the spatial scale analyzed, the remaining map-types tend to be more variable from one place to another. This variability could be due to local features, such as how zone 1 is much warmer during a type 7 event, due to being affected by slope flows off the Coast range. It is important to not only look at the broad view of how a particular map-type affects the region, but also locally for each individual climate zone.

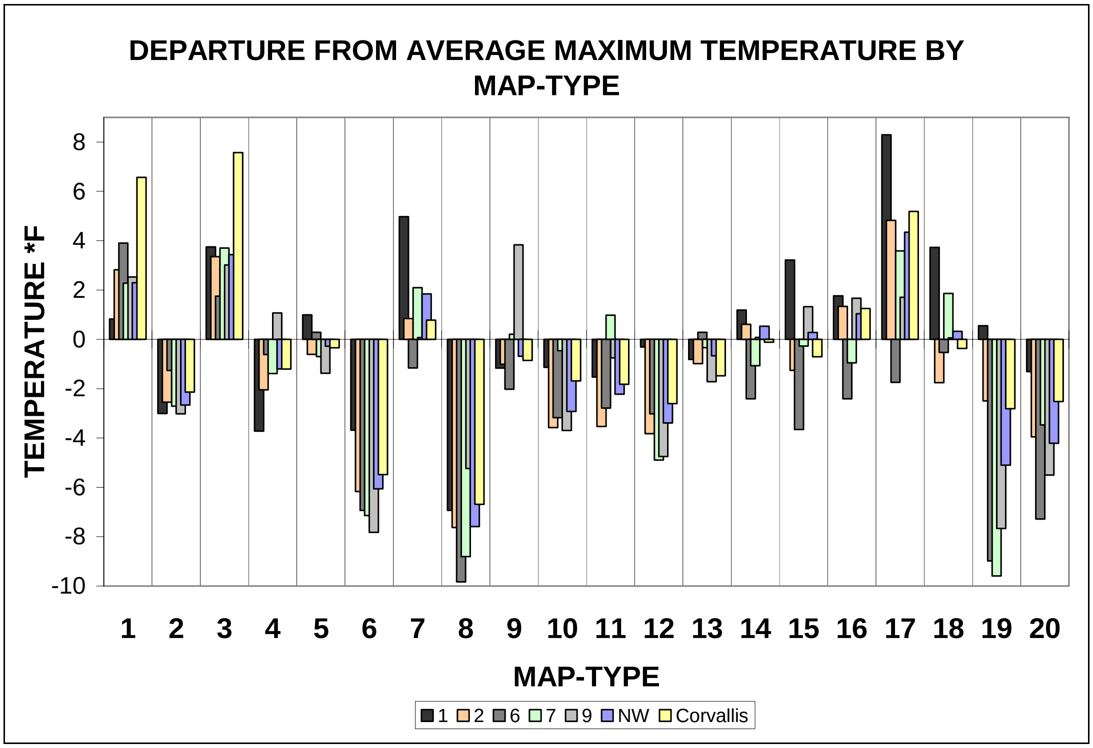

Figure 6.8: Shows the departure from the mean maximum temperature for climate zones 1, 2, 6, 7 and 9, NW average and Corvallis by map-type.

6.2 Minimum Temperature

The following analyses of minimum temperature are presented in the same way as was seen for maximum temperature.

6.2.1 NW Regional Averages

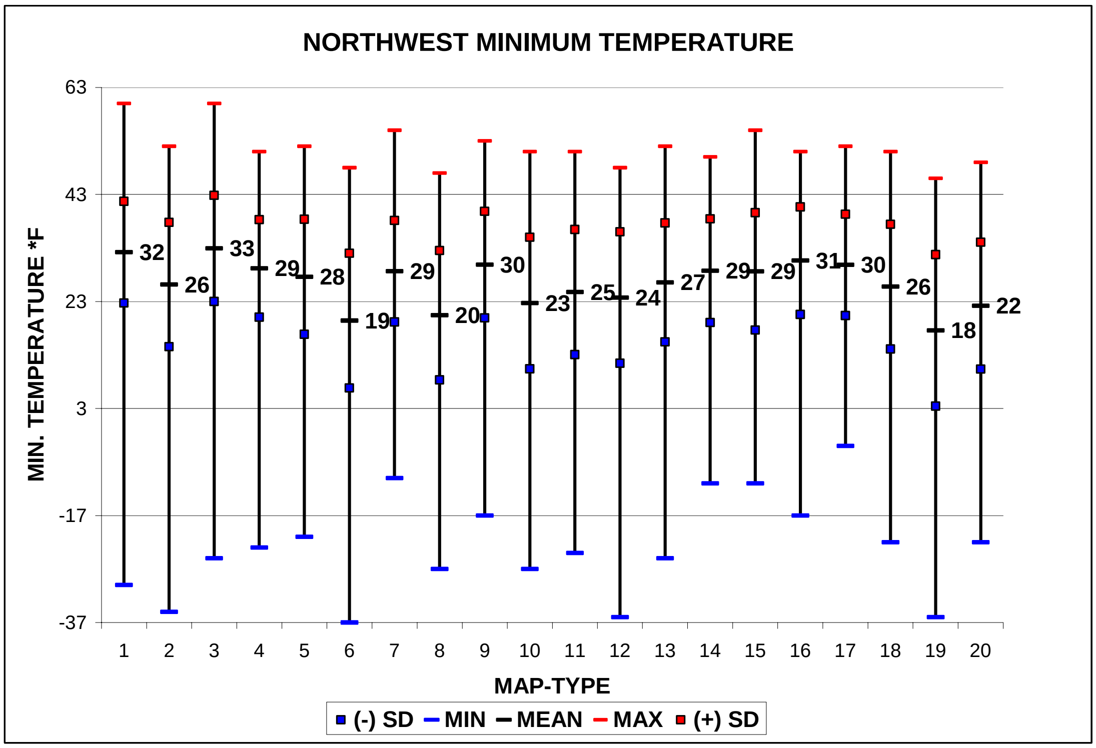

Figure 6.9: Northwest average minimum temperature by map-type.

Table 6-5: Corresponding values for Figure 6.9, showing the mean, standard deviation, minimum and maximum values for daily minimum temperature by map-type for the Pacific Northwest average.

	1	2	3	4	5	6	7	8	9	10	11	12	13	14	15	16	17	18	19	20
MEAN	32	26	33	29	28	19	29	20	30	23	25	24	27	29	29	31	30	26	18	22
SD	10	12	10	9	11	13	9	12	10	12	12	12	11	10	11	10	9	12	14	12
MIN	-30	-35	-25	-23	-21	-37	-10	-27	-17	-27	-24	-36	-25	-11	-11	-17	-4	-22	-36	-22
MAX	60	52	60	51	52	48	55	47	53	51	51	48	52	50	55	51	52	51	46	49

The warmest mean minimum temperature for the Northwest was found to be map-type 3 (see figure 6.10 b). The coldest mean minimum temperature was found with map-type 19 (see figure 6.10 a). There is just over a 15˚F difference between the warmest minimum temperature and the coldest minimum temperature. Map-types 3 and 19 contain flow from opposite directions; map-type 3 is from the southwest and map-type 19 is from the northeast.

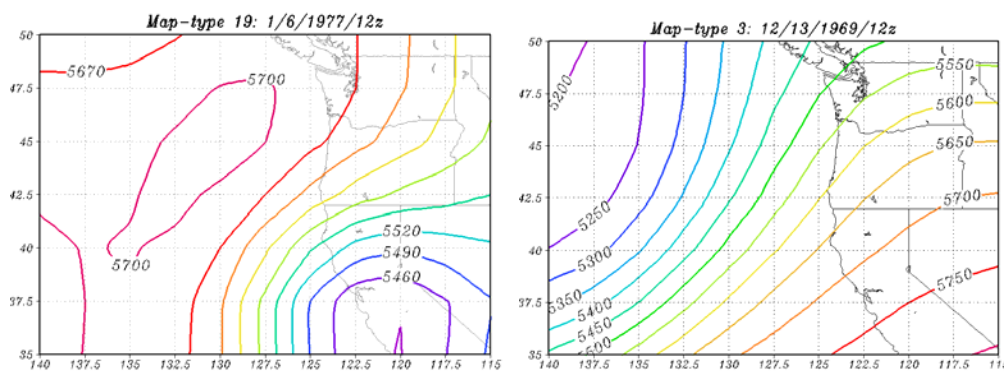

(a) *(b)*

Figure 6.10: (a) Map-type 19, the map-type with the NW coldest minimum temperature. (b) Map-type 3, the map-type with the NW warmest minimum temperature.

6.2.2 *Average Minimum Temperature by Oregon Climate Zone*

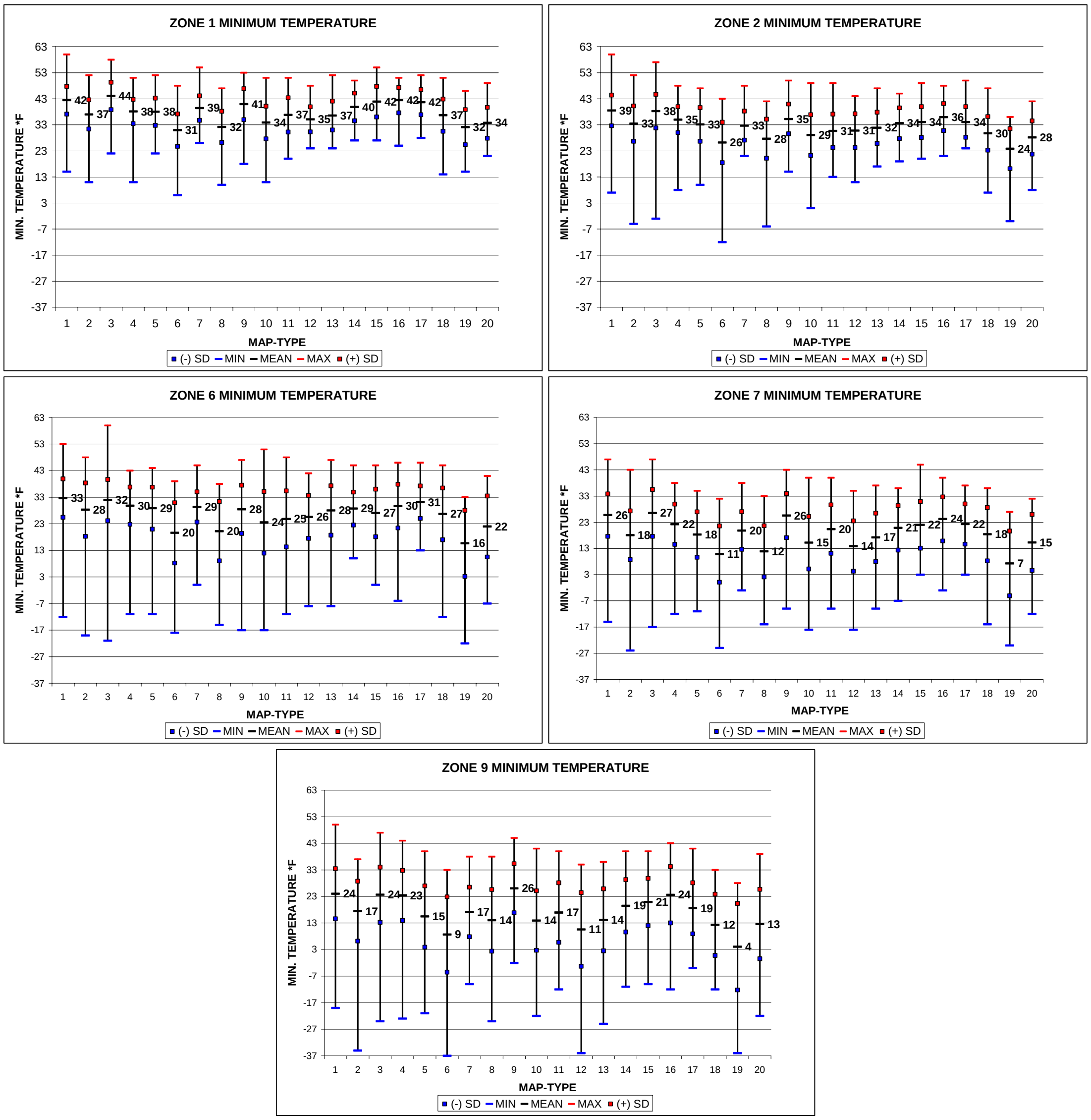

Figure 6.11: Oregon climate zones 1, 2, 6, 7, and 9 minimum temperature by map-type, including the mean, standard deviation maximum and minimum values.

Table 6-6: Coldest and warmest minimum temperature map-types.

	Coldest Map-type	Warmest Map-type
NW Average	19	3
Zone 1	6	3
Zone 2	19	1
Zone 6	19	1
Zone 7	19	3
Zone 9	19	9

As was seen with the analysis of maximum temperature, the coldest and warmest map-types are not the same in every zone. Figure 6.11 shows how the minimum temperature distribution varies for each climate zone. Map-type 3 is the warmest minimum temperature map-type in zones 1 and 7. In zones 2 and 6, the warmest map-type is 1, and in zone 9, the warmest map-type is 9. Each climate zone is affected by different aspects of the flow, not to mention other influences such as slope flows.

There is less variation in which map-type is associated with the coldest minimum temperature. Map-type 19 is the coldest overall amongst four of the five zones analyzed. In zone 1, map-type 6 is associated with the coldest mean minimum temperature, although, type 19 is only 1 degree warmer. Zone 1 tends to be milder than the other zones, as well as having the smallest standard deviation from the mean. This analysis shows that it is important to analyze each climate zone independently, recognizing the similarities and differences between both the range of values and correlations to minimum temperature.

6.2.3 Corvallis Averages

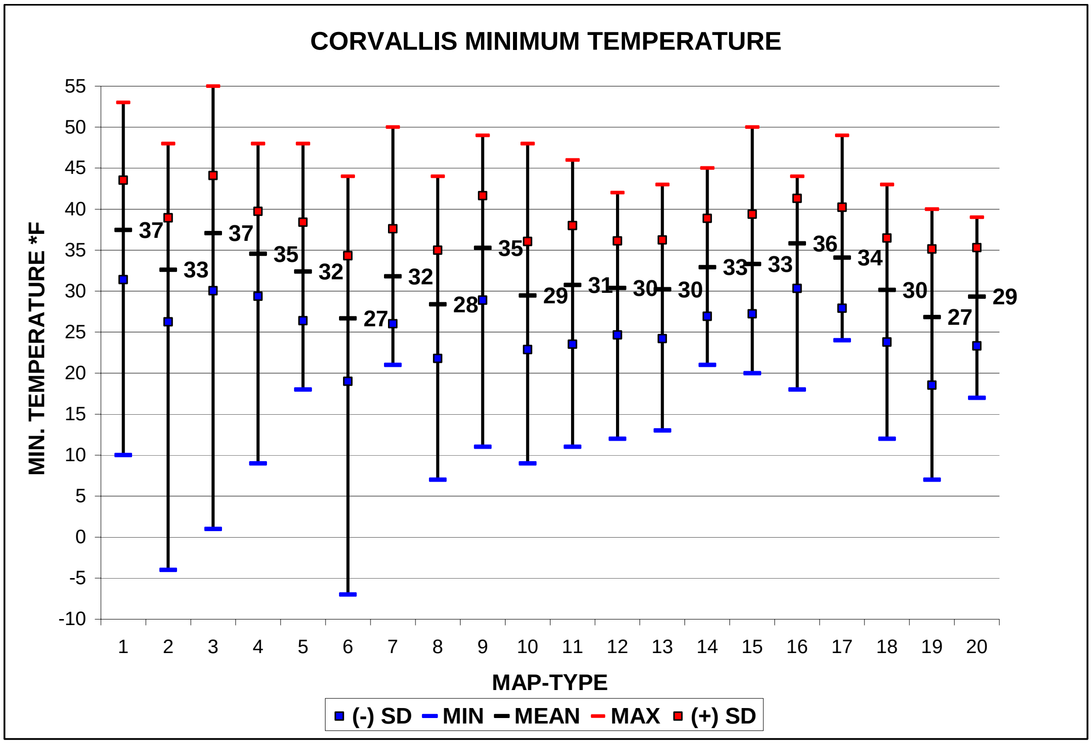

Figure 6.12: Average minimum temperature in Corvallis by map-type.

Table 6-7: Corresponding values for Figure 6.12, showing the mean, standard deviation, minimum and maximum values for daily minimum temperature by map-type for Corvallis.

	1	2	3	4	5	6	7	8	9	10	11	12	13	14	15	16	17	18	19	20
MEAN	37	33	37	35	32	27	32	28	35	29	31	30	30	33	33	36	34	30	27	29
SD	6	6	7	5	6	8	6	7	6	7	7	6	6	6	6	5	6	6	8	6
MIN	10	-4	1	9	18	-7	21	7	11	9	11	12	13	21	20	18	24	12	7	17
MAX	53	48	55	48	48	44	50	44	49	48	46	42	43	45	50	44	49	43	40	39

The Corvallis minimum temperature data is very similar to the zone data. The coldest mean minimum temperature map-type in Corvallis is type 6, although type 19, the coldest map-type for several of the Oregon climate zones is only about 0.1˚F warmer. The warmest minimum temperature map-type in Corvallis is type 1, which is almost 11˚F warmer than type 6, the coldest map-type. Map-type 3, the warmest map-type for some of the climate zones, is only about 0.4˚F colder than type 1. Map-type 6 consists of northerly flow over Corvallis and map-type 1 is westerly flow.

6.2.4 Corvallis Record Events

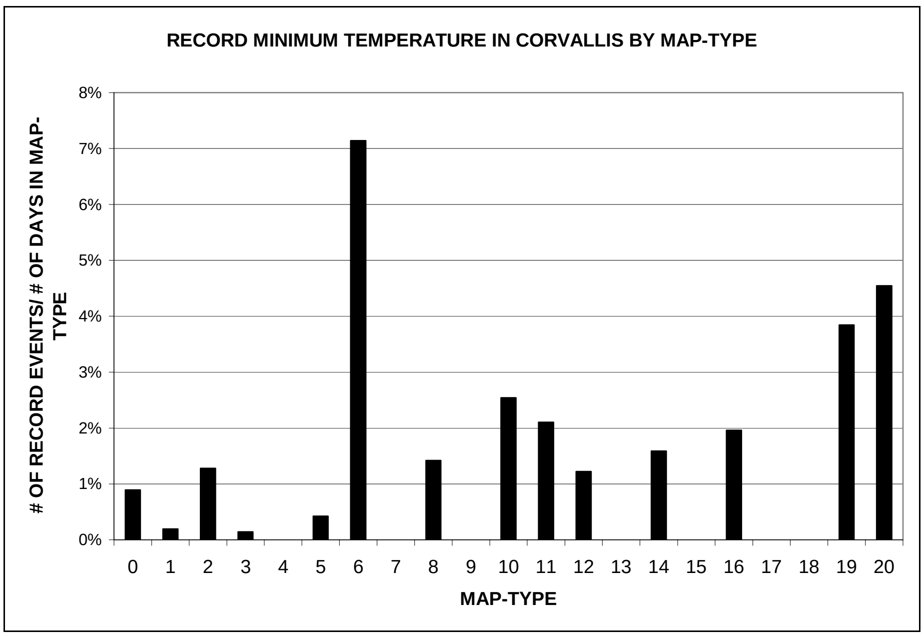

Figure 6.13: Normalized frequency of record minimum temperature in Corvallis by map-type, calculated by taking the # of record events in each map-type/ the number of days in each map-type. Only records that occurred after 1948 were included in the study.

When analyzing record minimum temperature in Corvallis, it is seen that 13 out of 20 map-types currently hold a record minimum temperature. However, a more close inspection reveals that 16 out of the 46 total days holding a record minimum temperature between 1948 and 2005 are found to be map-type 6, a northerly flow pattern. Map-type 6 was also the average coldest map-type in Corvallis.

6.2.5 Spatial Scale Comparison and the Departure from the Mean

Figure 6.14 summarizes the minimum temperature data. Each map-type's correlation to the minimum temperature closely resembles that which was seen with the maximum temperature data. Map-types 1 and 3 are the only types that are always warmer than average, and types 2, 5, 6, 7, 8, 10, 11, 12, 13, 18, 19, 20 are always colder than average, regardless of the spatial scale analyzed. The data for map-types 4, 9, 14, 15, 16 and 17 vary more between the zones, indicating either local differences affecting the main flow patterns or changes in the flow pattern from one zone to another.

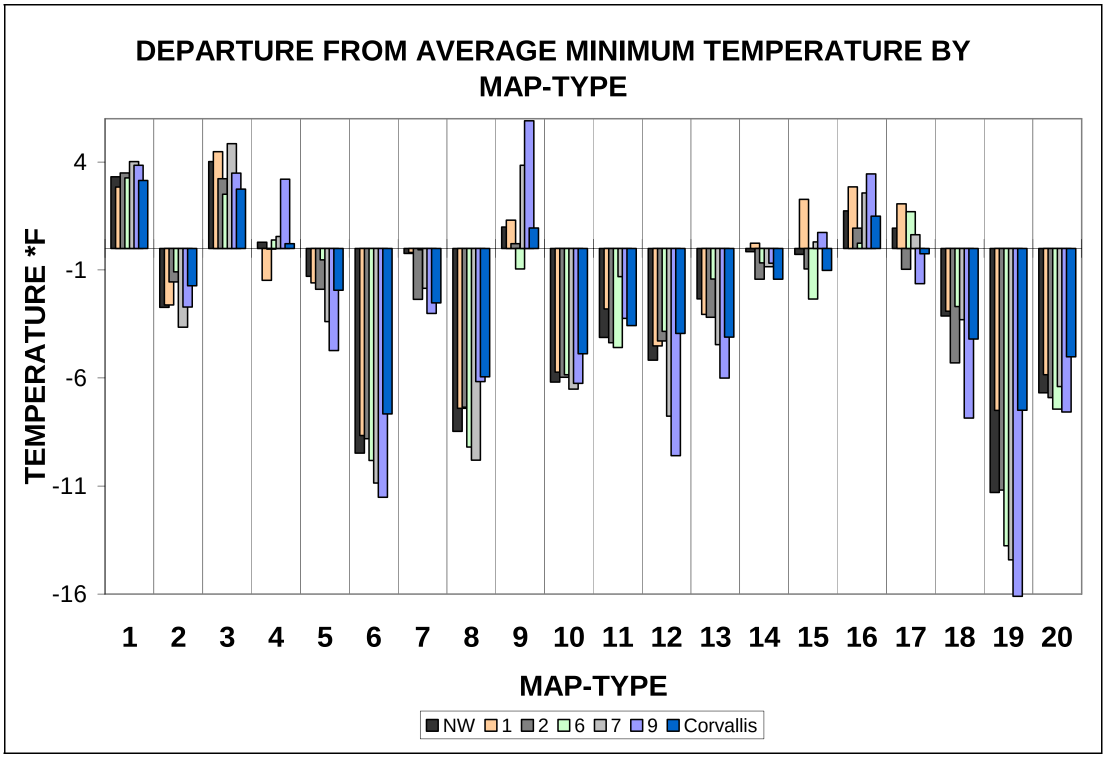

Figure 6.14: Shows the departure from the mean minimum temperature for climates zones 1, 2, 6, 7 and 9, NW average and Corvallis by map-type.

6.3 Precipitation

It is common knowledge that when air travels over water it will contain more moisture than had it traveled over land. Therefore, it is not a surprise that daily precipitation totals in the Pacific Northwest are highly influenced by map-type. The following results were calculated by the same methods as explained for maximum temperature and are presented in the same manner as in the previous two sections.

6.3.1 NW Regional Averages

Figure 6.15 shows the average amount of daily precipitation totals for each map-type. Several of the map-types have extreme rainfall maximums of more than two inches; however, all of the mean values fall below one half of an inch.

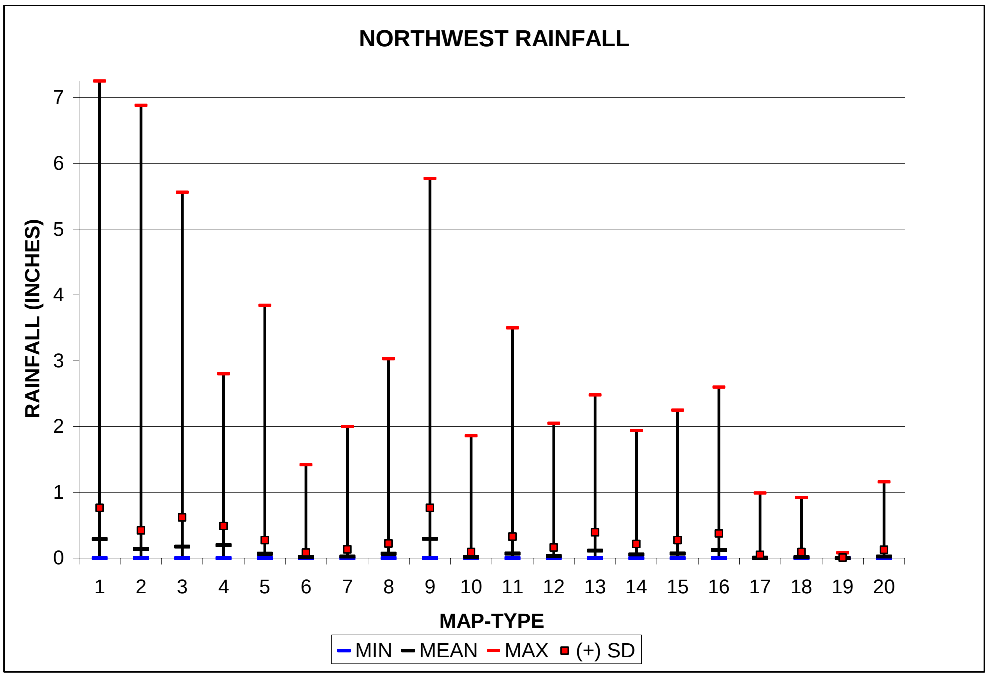

Figure 6.15: Northwest precipitation by map-type, including mean, min., max., and positive standard deviation.

Table 6-8: Corresponding values for Figure 6.15, showing the mean, standard deviation and maximum values for daily rainfall totals by map-type for the Pacific Northwest Average.

	1	2	3	4	5	6	7	8	9	10	11	12	13	14	15	16	17	18	19	20
MEAN	0.29	0.14	0.17	0.20	0.07	0.02	0.02	0.07	0.29	0.02	0.07	0.03	0.11	0.06	0.07	0.12	0.01	0.01	0.00	0.02
SD	0.47	0.28	0.44	0.29	0.21	0.07	0.11	0.16	0.47	0.08	0.26	0.13	0.28	0.16	0.20	0.25	0.05	0.08	0.01	0.10
MAX	7.25	6.88	5.56	2.80	3.84	1.42	2.00	3.03	5.77	1.86	3.50	2.05	2.48	1.94	2.25	2.60	0.99	0.92	0.08	1.16

As table 6-8 shows, map-type 9 produces the largest amount of precipitation (only about .003 inches more that type 1) while map-type 19 produces the least. As seen in figure 6.16 (a) and (b), map-type 9 is a southwesterly flow pattern and type 19 is a northeasterly flow pattern.

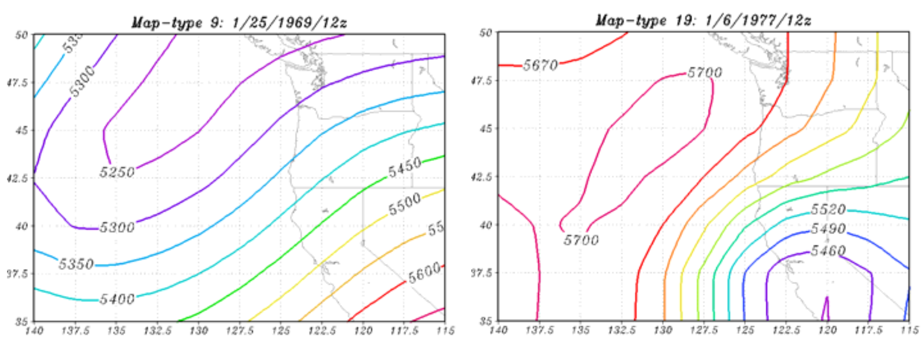

(a) (b)

Figure 6.16: (a) wettest map-type and (b) driest map-type

6.3.2 Average by Oregon Climate Zone

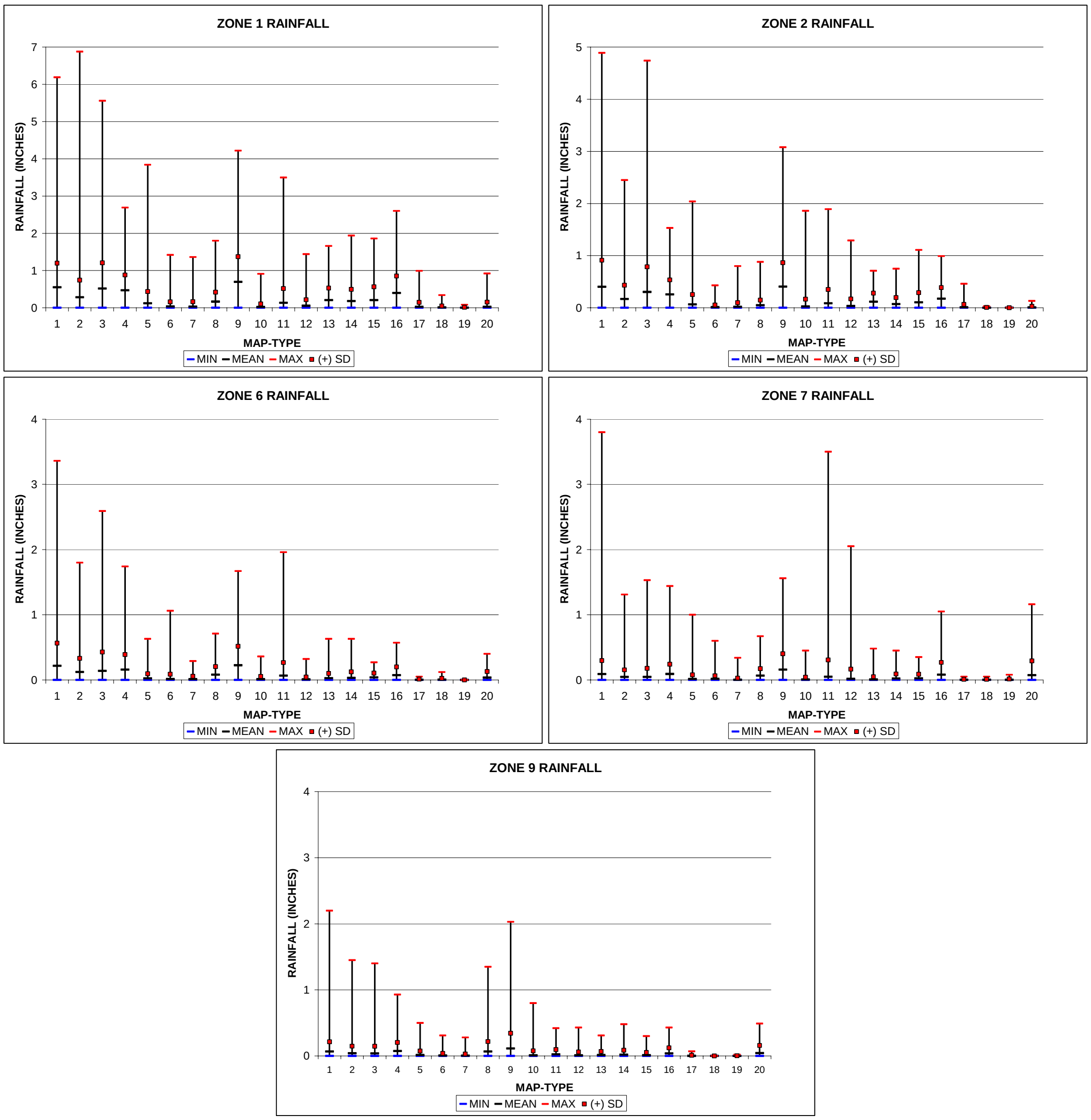

Figure 6.17: Precipitation by map-type in each zone, showing mean, positive standard deviation and maximum values.

The climate zone results are similar to the Northwest average data. Table 6-4 compares the wettest and driest maps from figure 6.17 and the Northwest as a whole. The wettest map-type was type 9 (see figure 6.16 (a)) for the Northwest average and all of the climate zones. The driest map-type was type 19 (see figure 6.16 (b)) for the Northwest average and zones 1, 2, and 6. Zones 7 and 9 had a different driest map-type, although type 19 was extremely dry as well.

Table 6-9: Wettest and driest map-types by climate zone.

	Wettest Map-type	Driest Map-type
NW Average	9	19
Zone 1	9	19
Zone 2	9	19
Zone 6	9	19
Zone 7	9	17
Zone 9	9	18

6.3.3 Corvallis Averages

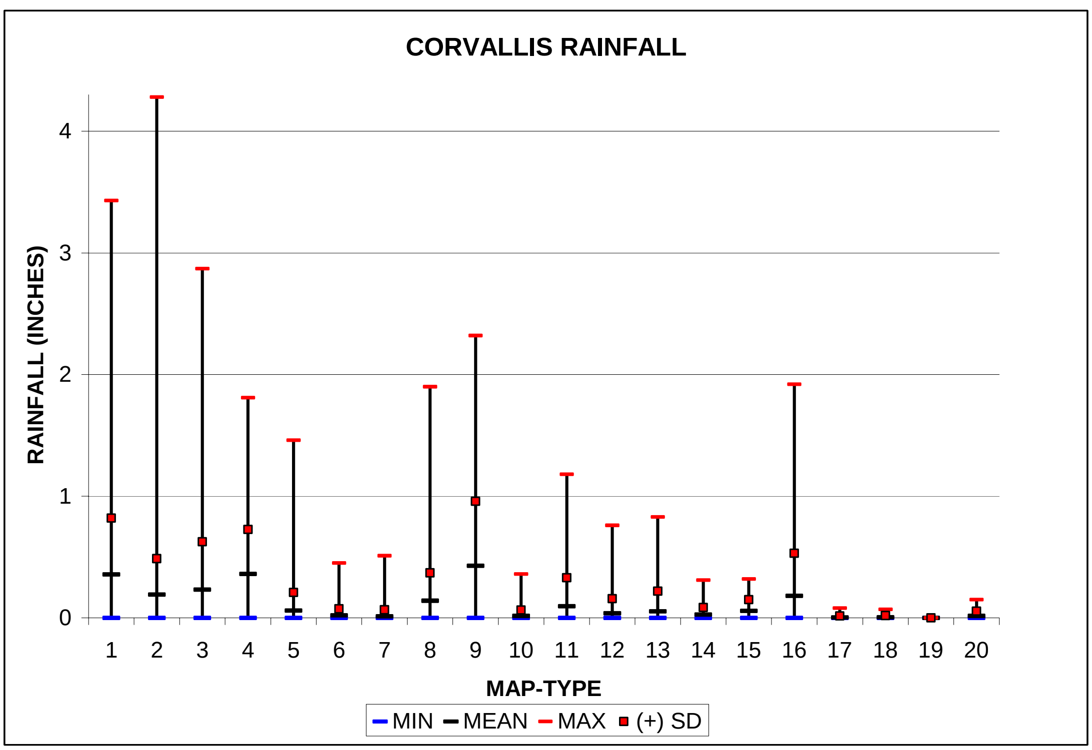

Figure 6.18: Precipitation in Corvallis by map-type showing mean, positive standard deviation, minimum and maximum values.

Table 6-10: Corresponding values for Figure 6.18, showing the mean, standard deviation and maximum values for daily rainfall totals by map-type for Corvallis.

	1	2	3	4	5	6	7	8	9	10	11	12	13	14	15	16	17	18	19	20
MEAN	0.36	0.19	0.23	0.36	0.06	0.02	0.01	0.14	0.43	0.02	0.09	0.04	0.05	0.03	0.06	0.18	0.00	0.00	0.00	0.02
SD	0.46	0.30	0.39	0.37	0.15	0.05	0.05	0.23	0.53	0.05	0.24	0.12	0.16	0.06	0.09	0.35	0.01	0.02	0.00	0.04
MAX	3.43	4.28	2.87	1.81	1.46	0.45	0.51	1.90	2.32	0.36	1.18	0.76	0.83	0.31	0.32	1.92	0.08	0.07	0.00	0.15

Figure 6.18 and table 6-10 show the wettest map-type in Corvallis is type 9 (see figure 6.16 (a)) and the driest map-type is 19 (see figure 6.16 (b)). For the period analyzed, there has never been recorded precipitation in Corvallis on a type 19 day. Precipitation proves to be very sensitive to map-type and the results seen in Corvallis are the same across the Northwest region.

6.3.4 Corvallis Record Events

When looking at which map-type group contains the most record daily precipitation events, the wettest map-type continues to stand out. Figure 6.19 shows that the greatest chance of record precipitation in Corvallis in winter occurs on a day with a type 9 map. All of the 56 record events that occurred during the winter months between 1948 and 2005 were associated with one of types 1, 2, 3, 4, 9, or 16. The remaining 14 map-types are not associated with any record rainfall events.

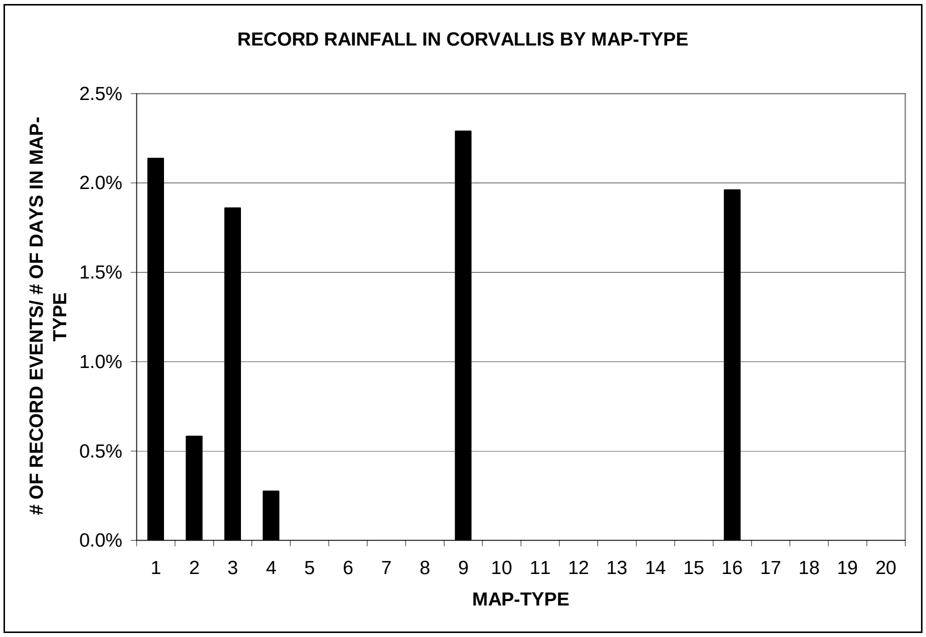

Figure 6.19: Normalized frequency of record precipitation in Corvallis by map-type, calculated by taking the # of record events in each map-type/ the number of days in each map-type. Only records that occurred after 1948 were included in the study.

6.3.5 Spatial Scale Comparison and the Departure from the Mean

Figure 6.20 shows the departure from average precipitation by map-type for each of the regions studied. It is quickly seen that wet map-types are typically wet and the dry map-types are typically dry, regardless of the spatial scale included in the study. However, each climate zone has an individual relationship to rainfall. For example, zone 1 tends to be more extreme and is highly influenced by the flow patterns, where zone 7 is more moderately affected.

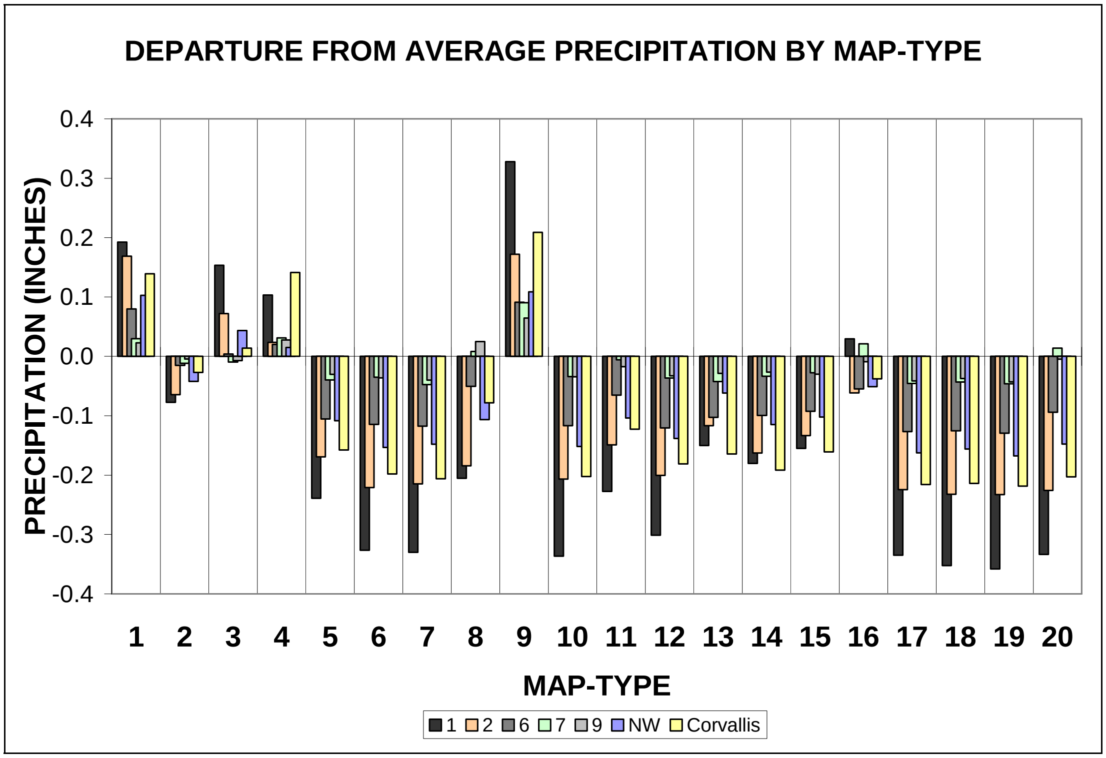

Figure 6.20: Departure from average precipitation by map-type and region.

6.4 Snow Fall

The occurrence of surface level snowfall is highly variable and is dependent on several factors. Figure 6.21 shows the relatively low correlation between the maximum snowfall values for each map-type and the mean values, indicating there are extreme outliers in the data. In order for snow to accumulate at the surface, the air mass must be cold and contain sufficient moisture, therefore one would expect the map-types which produce the most mean snowfall amounts in the Pacific Northwest to be a combination of the coldest types and moistest types found previously.

The snowfall data are presented in the same manner as the previous three sections.

6.4.1 NW Regional Averages

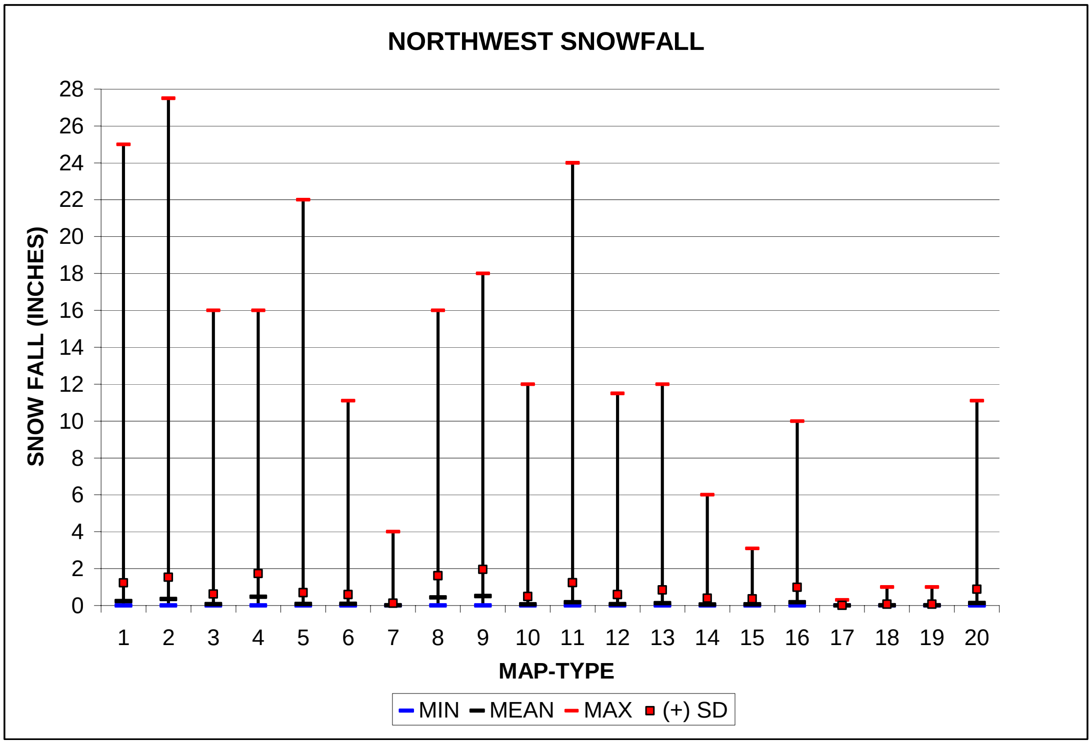

Figure 6.21: Northwest average snowfall by map-type

Table 6-11: Corresponding values for Figure 6.21, showing the mean, standard deviation and maximum values for daily snowfall totals by map-type for the Northwest average.

	1	2	3	4	5	6	7	8	9	10	11	12	13	14	15	16	17	18	19	20
MEAN	0.2	0.4	0.1	0.5	0.1	0.1	0.0	0.4	0.5	0.1	0.2	0.1	0.1	0.0	0.1	0.2	0.0	0.0	0.0	0.1
SD	1.0	1.2	0.5	1.3	0.6	0.5	0.1	1.2	1.5	0.4	1.1	0.5	0.7	0.4	0.3	0.8	0.0	0.1	0.1	0.8
MAX	25.0	27.5	16.0	16.0	22.0	11.1	4.0	16.0	18.0	12.0	24.0	11.5	12.0	6.0	3.1	10.0	0.3	1.0	1.0	11.1

For the Pacific Northwest as a whole, Figure 6.21 and Table 6-11 show that types 9, 4, and 8 are the top three map-types associated with snow; types 7, 17, 18 and 19 rarely generate snow. Type 9 was found previously to be associated with the greatest precipitation and type 8 was one of the coldest flow patterns. Type 4 was previously found to be the third wettest map-type and the ninth coldest map-type. Type 17 was previously found to be the warmest, type 19 was the driest and type 7 was the fourth warmest. A perfect balance between temperature and moisture must be in place for the possibility of significant snowfall.

6.4.2 Average snowfall by Oregon Climate Zone

The results for snowfall by map-type are similar to the Northwest data. Zones 1 and 2 have the smallest amount of snowfall in Oregon while zone 6 is typically associated with the most snowfall. Figure 6.22 and Table 6-5 show the breakdown of the map-types with the most and those with the least snow. Several map-types have never produced snow in some regions. Of important note is the scale of the charts in figure 6.22, all of the mean data points are below one inch, making the variability between map-types on an order of a tenth of an inch.

Table 6-12: Snowiest and least snowiest map-types. In the list of map-types associated with the least snow, all of the climate zones, except zone 7, have never had any recorded snow.

	Map-type with the most snow	**Map-type with the Least snow**
NW Average	9	17
Zone 1	4	5,7,14,15,16,17,18,19
Zone 2	4	7,17,18,19,20
Zone 6	8	19
Zone 7	8	17
Zone 9	8	17,18,19

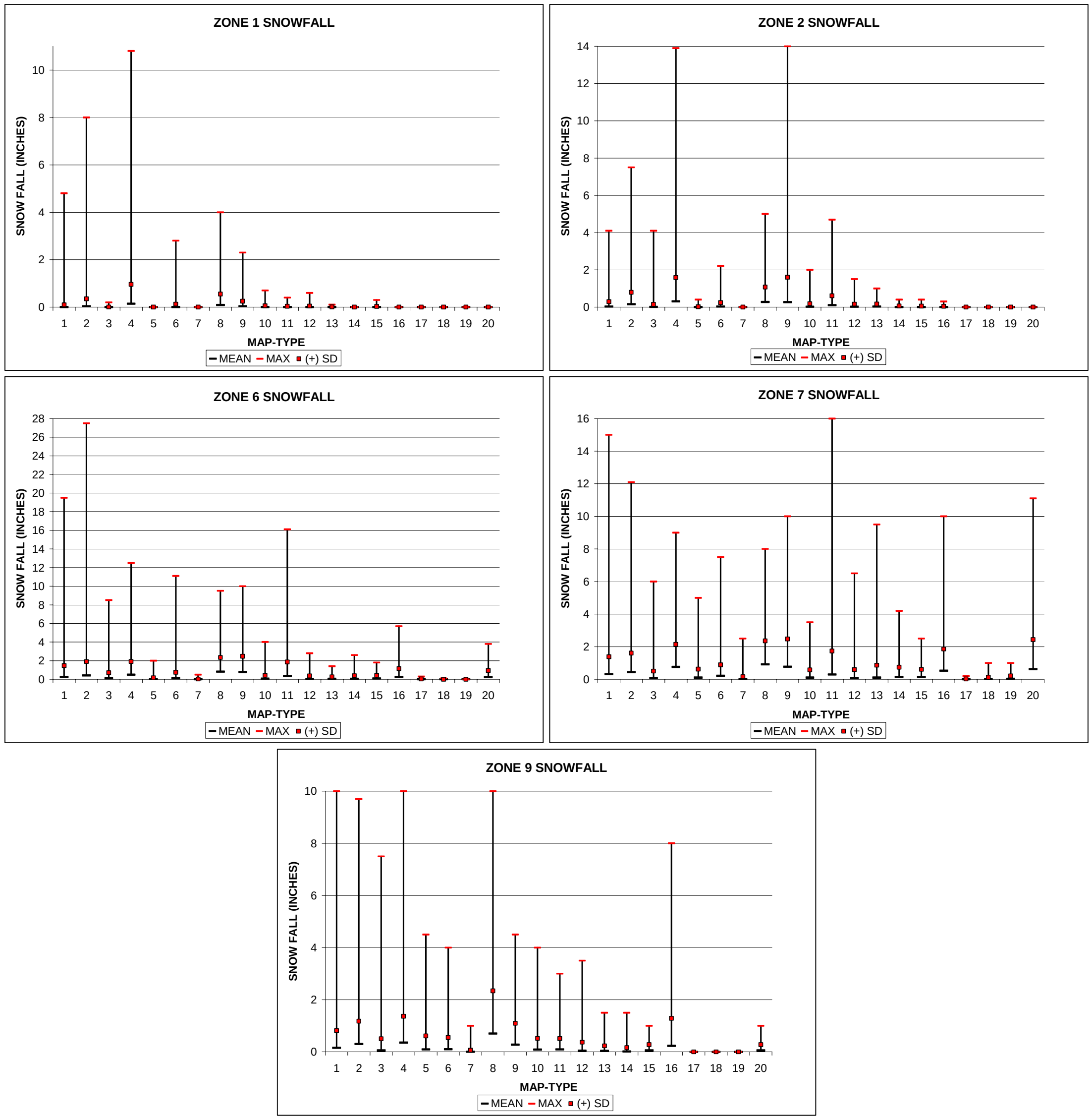

Figure 6.22: Average snowfall in each zone by map-type, including the mean, positive standard deviation and maximum values.

6.4.3 Corvallis Averages

Similar to the analysis of zone data, the Corvallis data show that map-types 8, 4 and 9 are the largest snow producers. Type 8 is a cold map-type with flow around a deep trough from the northeast, while type 9 is a wet type with flow around a deep trough from the southwest. Map-type 4 is mostly westerly flow with a small trough centered off the coast, although, on the type 4 days associated with snowfall, the trough shows up as more of a low-pressure center. The combinations of wet and cold map-types are thus seen to be associated with the Corvallis snowfall data.

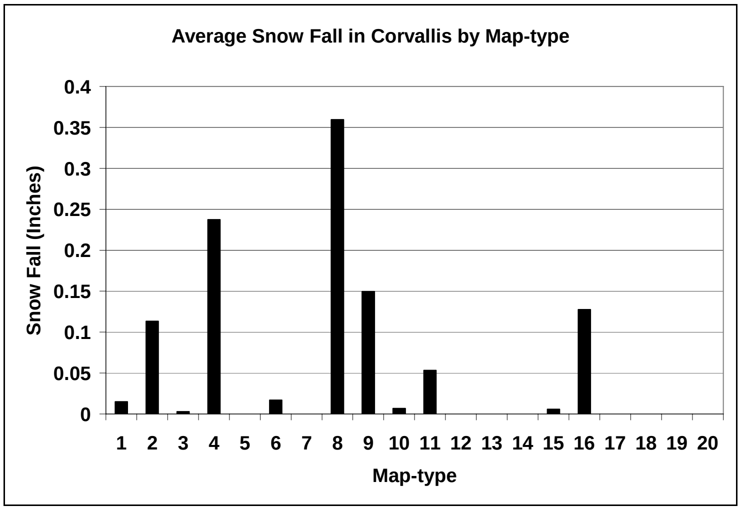

Figure 6.23: Average snowfall in Corvallis by Map-type.

6.4.4 Corvallis Record Snowfall Events

The Corvallis record snowfall data closely parallels the data seen above. Type 8 stands out as the biggest record snowfall producer. Type 16 shows up as being the fourth largest record event holder. However, since map-type 16 is rare, and was associated with only one large record event, its importance as a snow producer may be over-rated.

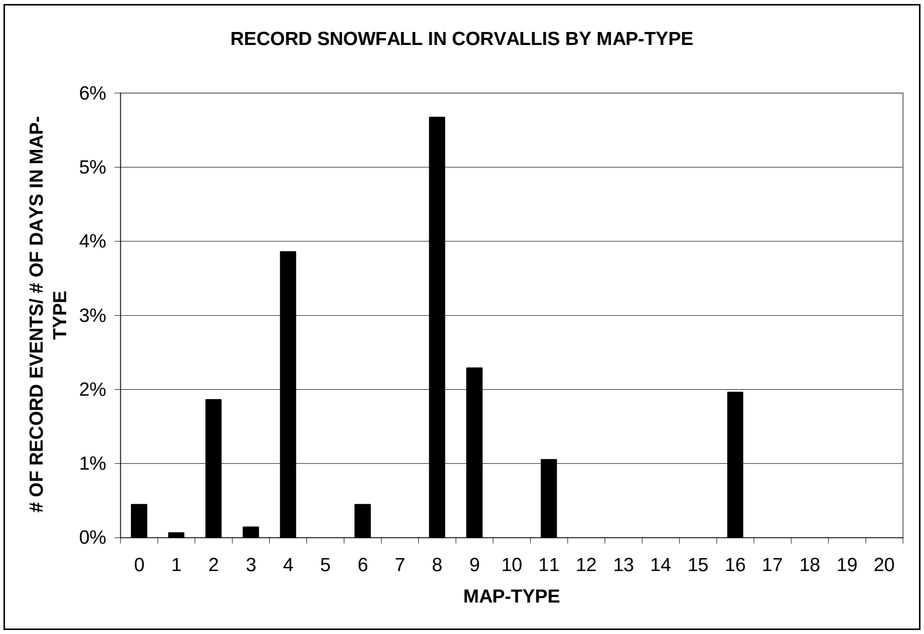

Figure 6.24: Normalized frequency of record snowfall in Corvallis by map-type, calculated by taking the # of record events in each map-type/ the number of days in each map-type. Only records that occurred after 1948 were included in the study.

6.4.5 Spatial Scale Comparison and the Departure from the Mean

Correlating snowfall data and map-types reiterates the large array of conditions needed to produce snow in areas similar to Corvallis. Even though the map-types that produce the largest snowfall can be quite different, there are only a handful that produce snow at all in areas such as Corvallis. Therefore, having a catalog of the snowiest events and the upper-air conditions can be quite useful. Figure 6.25 is a summary of all the regions studied, which again shows map-types 4, 8, and 9 as being the snowiest and types 17, 18 and 19 being the least snowiest.

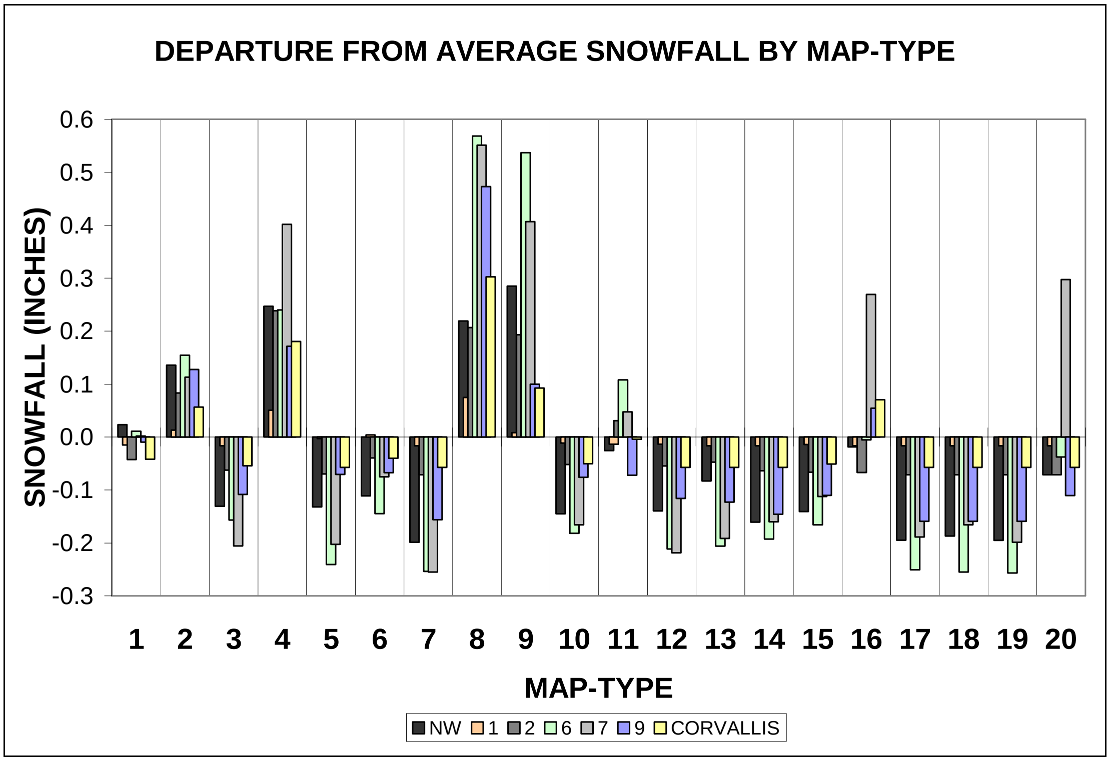

Figure 6.25: Departure from average snowfall by map-type.

6.5 El Niño and La Niña Years

Studies of weather during El Niño and La Niña events are of considerable interest as these events can lead to quite drastic differences in the weather elements observed at the surface. Knowing that synoptic map-pattern climatology relates atmospheric flow to surface weather data, it can be hypothesized that the map-type data reflect the differences in weather seen during an El Niño or La Niña year. In order to test this, the map-type data were divided into El Niño seasons, La Niña seasons or normal seasons based on the consensus list prepared by Golden Gate

Weather Services (Null 2004). This list is a composite of four major ENSO event lists established by the Western Regional Climate Center, Climate Diagnostics Center, Climate Prediction Center and the Multivariate ENSO Index from the Climate Diagnostics Center. Figure 6.26 shows the distribution of map-types for El Niño seasons and La Niña seasons compared to the distribution for the entire dataset (drawn as a curve for clarity).

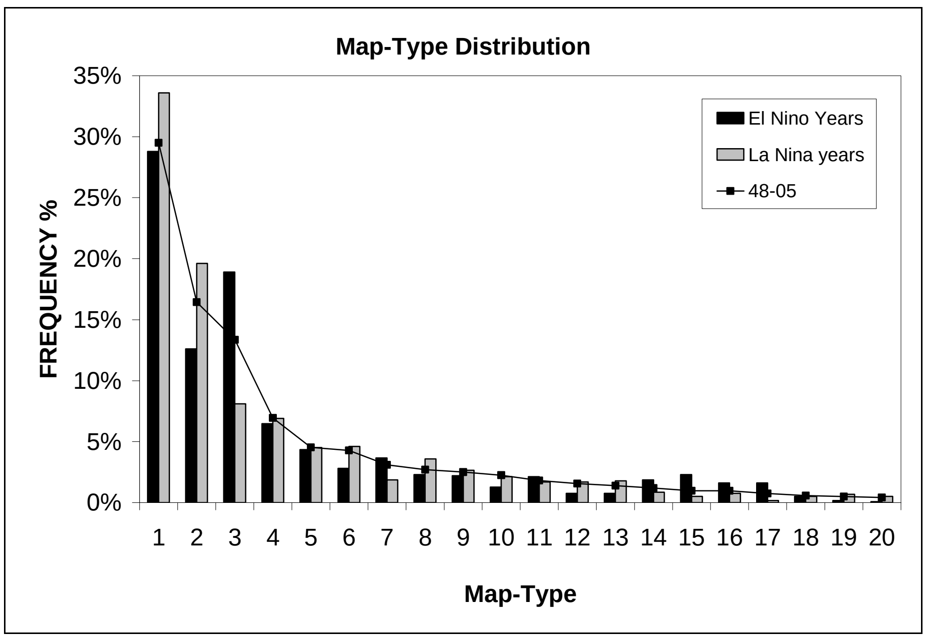

Figure 6.26: Comparison of the distribution of map-types for El Nino years, La Nina years, and the entire data set (drawn as a curve for clarity).

The figure shows that map-types 2 and 3 occur with quite different frequencies in El Niña and La Niña years (ENSO events). During La Niña years there are more type 2 maps than average, but less type 3 maps. El Niño years have just the opposite, less type 2 maps, but more type 3 maps. Recalling from the previous sections, map-type 2 is typically a colder flow pattern where type 3 is one of the warmest flow patterns.

The changes in the frequencies of flow types that occur aloft (as revealed by the map-types) directly affect the weather that occurs at the surface. Analyzing temperature and precipitation shows the warmest recorded winter season in 7 out of 9 climate zones in Oregon was during an El Niño year (1957-58). Figure 6.27 shows the distribution of map-types that year. During the 1957-58 season, there were several more types 1, 3, and 7 than compared to the long-term distribution of non-El Niño or non-La Niña years.

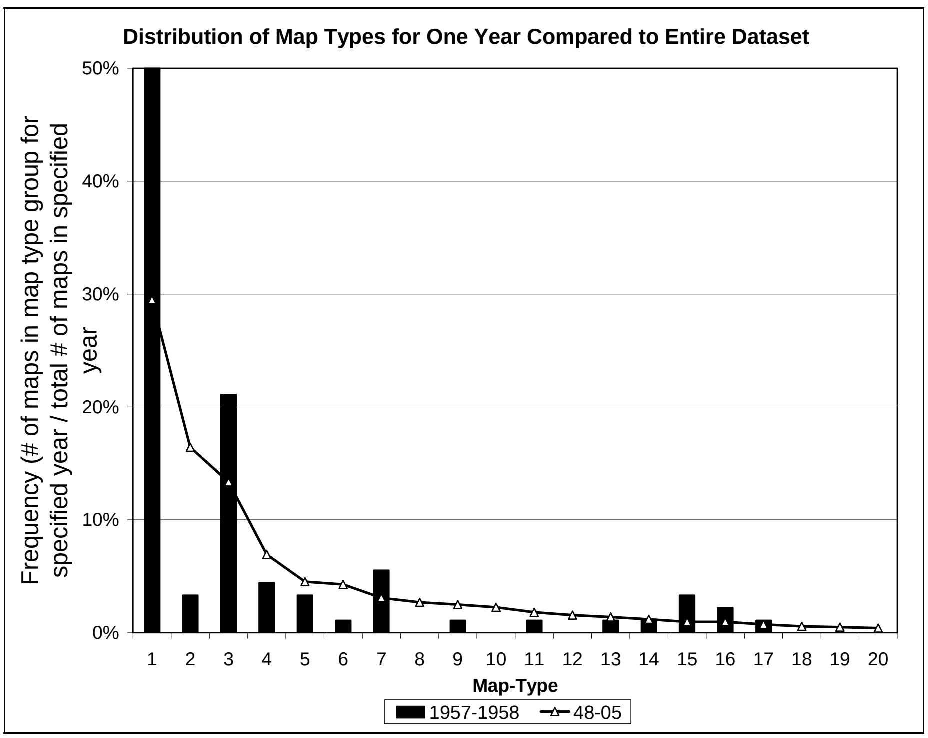

Figure 6.27: Distribution of map-types during 1957-1958 season compared to normal.

Figure 6.28 shows these three map-types are all warmer than average in the Pacific Northwest.

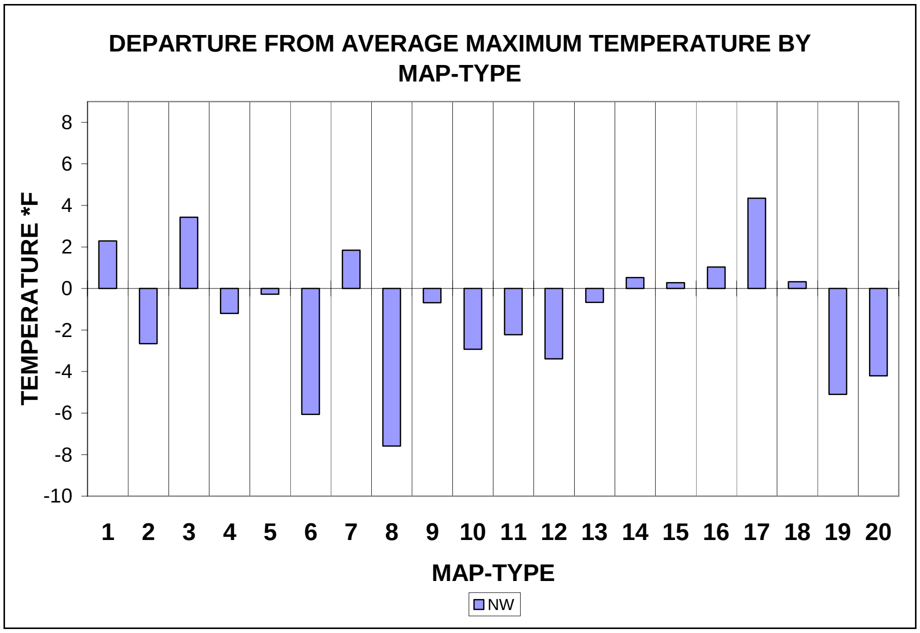

Figure 6.28: Departure from average maximum temperature for the Pacific Northwest, showing map-types 1, 3 and 7 are all warmer than average.

La Niña events also have a large impact on the weather at the surface. The wettest winter season for 5 out of 9 Oregon climate zones was during a La Niña season (1964-65). Figure 6.29 shows the distribution of map-types during this year.

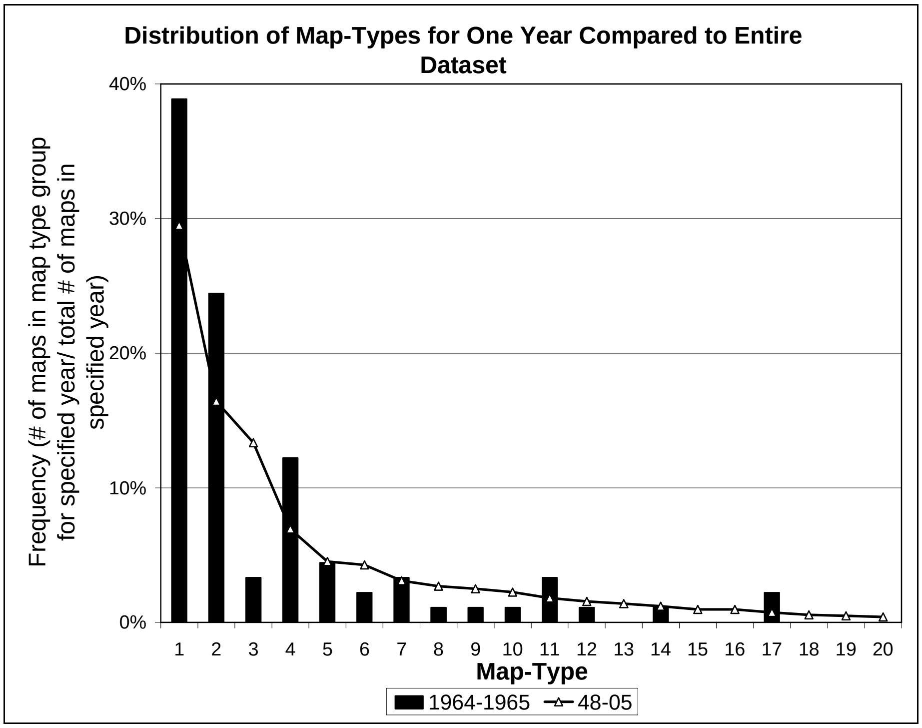

Figure 6.29: Distribution of map-types during 1964-65 season compared to normal. This distribution shows types 1, 2, and 4 occurred more often than normal.

These three types are three of the top five wettest map-types in the Pacific Northwest. It is also notable that many map-types occurred less than normal. Map-types 6, 10, 12, 18, and 19 are all very dry map-types, and they occurred less frequently.

Correlating El Niño and La Niña years to the map-type data shows the strong connection between the surface weather elements and atmospheric flow. Previous studies have already shown that, typically, El Niño years bring warmer than average conditions to the Pacific Northwest, and La Niña years bring wetter than average conditions ("El Nino and La Nina" 2006); this study emphasizes those conclusions and demonstrates the differences that are occurring aloft during El Niño or La Niña years.

Creating a synoptic climatology is truly a two-step process. Having a catalog of flow patterns only becomes significant once it is correlated to surface data. Countless variables and conditions at the surface could be correlated to map-type data to help understand the connections that may or may not be present. For the purposes of this study, the weather elements of temperature, precipitation, snowfall, and ENSO events were all well correlated to the map-type data, each proving to have a strong connection with the flow patterns aloft.

7 DISCUSSION AND CONCLUSIONS

The field of weather forecasting is as dynamic as the atmosphere; those who seek to understand the many relationships between the atmosphere and surface level processes have a long road ahead of them. Improving the accuracy of forecasting methods is a continual process as new tools are being discovered and the current forecasting tools are being improved. Many forecasters rely heavily on their experience with the weather of a particular region to supplement and support the forecasting tools they use. The experience one gains from forecasting in a particular region for an extended period can be valuable to the accuracy of their forecasting, however, one's experience is highly subjective and variable from one forecaster to another. Employing increased accessibility of weather data and improvements in computer technology, this study has used a long-standing method in a new way. A synoptic map-pattern climatology, such as the one described in this thesis, can provide weather forecasters with a historical view of the relationship between atmospheric circulations and surface level weather for any given region.

The correlation-based map-pattern climatology method first introduced by Lund in 1963 provides an objective and automated way of classifying atmospheric circulations and flow patterns into distinct categories, which can then be correlated to surface level weather data. This method is well researched and can now be effectively used given the amount and accuracy of weather data available and the vast improvements in computer capabilities. Lund's method was chosen because of its ease of use and ability to be reproduced. The map-typing results are actual upper-air charts that are easily read and understood. Although automated, easy to use and repeatable, this method is not completely objective, there are a few parameters that must be set in advance; the user must define the research area, correlation coefficient cutoff value, and the number of map-type groups found.

The research area chosen for this project was one that focused on a single region of the United States, being the Pacific Northwest. The research area had to be large enough to recognize the circulation patterns that affect the weather of the Pacific Northwest, while remaining small enough to ignore features not affecting this region. The domain chosen for this study was 15˚ by 25˚, although, if one were to use this method for a different region, the domain size would need to be reanalyzed and chosen based on the circulation patterns affecting that region.

After choosing the research area, Lund's method can then be applied, although the correlation coefficient 'critical value' and the number of map-type groups classified must be pre-determined. Typically, a critical value between 0.7 and 0.9 is chosen for correlation based map-pattern climatologies. Sabin (1974) found 0.8 to be the best critical value, allowing for a large number of map categories while still keeping a distinct and individual flow pattern for each category; 0.8 was also chosen for this study to allow for this balance. When creating the climatology, a set limit of map-types can be found, only recognizing the most common map-types or all of the possible map-type groups can be found. For this climatology, when a limit was not set, a total of 53 map-type groups were found. Recognizing all of the possible map-type groups allows for a thorough analysis of all of the possible flow patterns that occur in the Pacific Northwest, however this is far too many map-types to realistically correlate to surface weather data. In analyzing the less frequent map-type groups, it was found that many of the maps were essentially subsets of one of the more common map-type groups. For this study, a limit was set to only allow the 20 most common map-types to be classified. When a limit is set on how many map-type groups are found, there are fewer map-type groups each containing more maps, as well as a larger unclassified number of maps. Maps that originally made up their own group when no limit was set, are then grouped together with one of the more common map-types that they are also significantly correlated to when a limit is set. The smaller set of map-types can more-easily be analyzed and correlated to surface level weather data. A limit can be set in many ways. For this study, it was believed that 20 map-types provided a thorough representation of the significant flow patterns that occur in this region. An alternative could be to require a minimum percentage of the total maps to be in each group. Choosing the number of map-types to analyze is an important step in creating a map-pattern climatology and is dependent on the region and purpose of the climatology. Further research should be done in this area to determine what number of map-type groups provides the best representation of the circulation patterns that occur. Researching this number would require close attention to how each of the circulation patterns affect the surface environment and how different the types are from other groups in the dataset.

Although Lund's method is automated and easily executed, a significant downfall is the limitations of the Pearson product moment correlation equation. Using this correlation equation provides an excellent way to recognize similar map patterns, although it does not recognize magnitude differences from one map to another. The magnitudes of the patterns do have an impact on the resulting weather at the surface and therefore should be taken into consideration. To avoid any large shifts in the magnitude of the mean height field, this study limited the data to a single season, therefore avoiding the seasonal variability in pressure tendency. When correlating the map-types to surface level weather it is important to pay attention to any shifts in magnitude that may be taking place within a particular map-type as it may have an impact on the resulting weather.

This synoptic map-pattern climatology of the Pacific Northwest identified the 20 most common flow patterns that occur over this region during the winter months, along with a catalog of the corresponding weather occurring at the surface. Though this study only analyzes the winter season, the other seasons could easily be looked at in the same way. Temperature, precipitation and snowfall data were all correlated to the map-type data, providing a historical record of weather occurring at the surface during any of the 20 distinct flow patterns. The variables studied were chosen based on accessibility as they are all recorded daily at each weather station, although, other variables such as wind and fog could be correlated to the map-type data as well.

When looking at the temperature and precipitation data it was easily seen which map-types were wetter than average and which were warmer than average.

Any longtime resident of the Pacific Northwest would not be surprised by the correlations that were found between atmospheric circulations and surface weather data. Although, someone who is not as familiar with this region may find it interesting to be aware of the strong influence of westerly flow and the sharp contrast that exists between a westerly flow pattern and one with an easterly influence.

Record data were also correlated to the map-type data, showing which flow patterns have the greatest chance of producing a record event in temperature, precipitation or snowfall. The correlations between the record data and the map-type data were quite revealing, showing the most extreme map-types. Further statistical analysis could easily be done to recognize the risks associated with the more extreme map-types, not only to help weather forecasters better predict the extreme events, but also to provide analysis for the many groups affected by those extreme events. The department of transportation, water resource agencies, insurance companies, fire fighters, agricultural producers, and many others are significantly affected during extreme weather events and are continuously seeking to be better prepared physically and financially. If given more detailed statistical analysis about the correlation between extreme weather events and map-types, these groups would have a better understanding of what has happened historically and would therefore be able to better evaluate the risk associated with record events and be better prepared.

In addition to researching the historical averages of temperature, precipitation and snowfall, the distribution of map-types during El Niño and La Niña years was also analyzed in combination with the weather data from the surface. El Niño and La Niña years proved to have quite different map-type distributions compared to 'normal' years and the weather resulting at the surface was quite different as well. The connections between the atmosphere and the surface made in this study serve as examples of the types of data that could be provided to forecasters on a regular basis.

In order to truly be made available to forecasters, a synoptic climatology such as this would need to be distributed in an electronic format in which current atmospheric flow data is compared to historical data. It would be necessary to know today's projected map-type along with all of the historical surface weather data associated with that map-type in order for this information to replace the previously relied upon experiential knowledge. If distributed in this way, weather forecasters, could easily quantify what has happened historically with any given map-type, thus replacing their variable and subjective experiential knowledge with an objective and accurate record.

REFERENCES

Ahrens, C. D. (2000). Meteorology Today. Pacific Grove, Brooks/Cole.

Barry, R. G. and A. H. Perry (1973). Synoptic Climatology: Methods and Applications. London, Methuen and Co Ltd.

Bischoff, S. A. and W. M. Vargas (2003). "The 500 and 1000 hPa weather type circulations and their relationship with some extreme climatic conditions over southern South America." International Journal of Climatology **23**(5): 541-556.

Brinkmann, W. A. R. (1999). "Within-type variability of 700 hPa winter circulation patterns over the Lake Superior basin." International Journal of Climatology **19**(1): 41-58.

Court, A. (1957). "CLIMATOLOGY: COMPLEX, DYNAMIC, AND SYNOPTIC." Annals of the Association of American Geographers **47**(2): 125-136.

El Nino and La Nina (2006). National Weather Service Climate Prediction Center **2007**.

Hernandez, G. (2001). WEATHER IMPACT ON USA ECONOMY. NOAA Magazine Online.

Hoard, D. E. and J. T. Lee (1986). "Synoptic Classification of a Ten-Year Record of 500 mb Weather Maps for the Western United States." Meteorology and Atmospheric Physics **35**(1-2): 96-102.

Jacobs, W. C. (1947). "Wartime Developments in Applied Climatology." Meteorological Monographs **1**(1): 1-52.

Kistler, R., E. Kalnay, et al. (2001). "The NCEP–NCAR 50-Year Reanalysis: Monthly Means CD-ROM and Documentation." Bulletin of the American Meteorological Society **82**(2): 247-268.

Lund, I. A. (1963). "Map-Pattern Classification by Statistical Methods." Journal of Applied Meteorology **2**(Feb. 1963): 56-66.

Null, J. (2004). El Nino and La Nina Years: A Consensus List, Golden Gate Weather Services. **2006**.

Paegle, J. N. and L. P. Kierulff (1974). "Synoptic Climatology of 500-mb Winter Flow Types." Journal of Applied Meteorology **13**: 205-212.

Schoof, J. T. and S. C. Pryor (2004). "An evaluation of two GCMS: North American Teleconnections and Synoptic Phenomena."

Serreze, M. C. and A. J. Etringer (2003). "Precipitation characteristics of the Eurasian Arctic drainage system." International Journal of Climatology **23**(11): 1267-1291.

Wallace, J. M. and P. V. Hobbs (1977). Atmospheric Science an Introductory Survey. San Diego, Academic Press.

Weiher, R. (2006). Economic Statistics for NOAA. Washington D.C., National Oceanic and Atmospheric Sciences Administration**:** 1-67.

Willmott, C. J. (1987). "Synoptic Weather-Map Classification: Correlation versus Sums-of-squares." Professional Geographers **39**(2): 205-207.

Yarnal, B. (1993). Synoptic Climatology in Environmental Analysis. Boca Raton, Florida, Belhaven Press.

Yarnal, B., A. Comrie, et al. (2002). "Developments and Prospects in Synoptic Climatology." International Journal of Climatology **21**(15): 1923-1950.